

Just Say the Name: Online Continual Learning with Category Names Only via Data Generation

Minhyuk Seo¹, Diganta Misra^{2,3}, Seongwon Cho¹, Minjae Lee¹, and Jonghyun Choi⁴

¹ Yonsei University

{dbd0508, poiuy98749, reccos1020}@yonsei.ac.kr

² Carnegie Mellon University

³ Mila - Quebec AI Institute

diganta.misra@mila.quebec

⁴ Seoul National University

jonghyunchoi@snu.ac.kr

Abstract. In real-world scenarios, extensive manual annotation for continual learning is impractical due to prohibitive costs. Although prior arts, influenced by large-scale webly supervised training, suggest leveraging web-scraped data in continual learning, this poses challenges such as data imbalance, usage restrictions, and privacy concerns. Addressing the risks of continual webly supervised training, we present an online continual learning framework—‘**Generative Name only Continual Learning**’ (**G-NoCL**). G-NoCL uses a prompt refiner module ψ and a set of generators \mathcal{G} along with the learner f_θ . Moreover, G-NoCL employs a novel sample complexity-guided data ensembling technique to optimally sample training data from generated data from each generative model. Through extensive experiments, we demonstrate that our proposed (**G-NoCL**) significantly outperforms naive generator-ensembling, web-supervised, and even manually annotated data in both In-Distribution (ID) and Out-of-Distribution (OOD) generalization evaluations. Generated dataset we used are available at https://huggingface.co/datasets/seongwon980/Nameonly_generated.

Keywords: Continual Learning · Online Learning · Generative Model

1 Introduction

In the real-world scenario of continual learning (CL), data arrive in a streaming manner [3, 65], contrary to the offline setup where data are presented in substantial chunks corresponding to tasks or datasets. Despite the gradual improvement in the performance of online CL methods, existing studies often make the assumption of having abundant curated and annotated data. However, acquiring high-quality data in real-time poses significant challenges, particularly due to the necessity of annotating unlabeled stream data, which are essential but expensive [94, 125]. For example, in the McQueen dataset [136], label annotation cost 6,000 USD over 10 weeks. Despite recent advancements in unsupervised CL



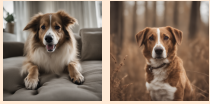


	Manually Annotated	Web Scraped	Generated
Dog			
	Cat		
Controllability		✗	○
Storage issues	Yes	No	No
Usage restrictions	No	Yes	No
Privacy issues	No	Yes	No
Acquisition cost	↑	↓	↓
Noise	↓	↑	↓

Fig. 1: Generated data addresses various constraints associated with web scraping or manually annotated data, effectively mitigating privacy concerns and usage restrictions, which refers to whether images can be used for learning. Simultaneously, it maintains controllability, which encompasses the ability to generate or acquire images with various contexts (e.g., background, color) as desired. Generated data is less noisy than web-scraped data and proves to be a more cost-effective acquisition method than manually annotated data which requires human annotation. Please refer to the supplementary material for details about the terms used in this figure.

approaches [78], which eliminate the need for labeled data, they often assume that the unlabeled data stream only includes data for the concepts⁵ to be learned (i.e., target concepts). However, in real-world scenarios, data unrelated to target concepts often coexist with relevant data streams. In addition to annotation cost, stream data often include privacy-sensitive images, which should not be utilized for model training purposes.

As an alternative to human-annotated data, recent studies [94, 106] use web-scraped data for online learning. Although web data presents advantages such as abundance [132], diversity [1], and easy accessibility [119], challenges arise from inherent noise [71, 84, 87], as well as privacy and copyright concerns [138], which pose obstacles for real-time training with web data. Moreover, incorporating web data judiciously necessitates the involvement of human annotators, which is similar to the requirements for labeled data. For example, DomainNet [84], a prominent benchmark in domain generalization, utilized web-scraped data, involving 20 human annotators who collaboratively dedicated a total of 2500 hours.

To overcome the limitations of both manual annotations and web-scraped data, we propose integrating a text-to-image (T2I) generative model with the online continual learner. T2I models provide controllability [86] and unlimited image generation capabilities [74], as illustrated in Fig. 1. However, T2I models suffer from finite diversity [14, 40, 122]. To improve *intra-diversity*, the diversity of images generated from a generator, we generate a diverse set of text prompts,

⁵The term *concepts* can be interchangeably used with categories or classes.

leveraging the in-context learning capability of Language Models (LLMs). Furthermore, we improve the *inter-diversity*, diversity of the generated images by ensembling the outputs of multiple T2I models, guided by a novel complexity-guided data ensembling, named DiverSity and COmplexity enhancing ensemble BIER (**DISCOBER**). Our empirical findings demonstrate that DISCOBER significantly boosts performance, while other ensemble methods often underperform compared to using a single T2I model.

In CL evaluation, the prevalent assumption is that training and test data adhere to *independent and identically distributed* (i.i.d.) principles. However, this assumption may not hold in real-world scenarios. In the case of training a model for autonomous driving, the available data may not cover all operational domains, leading to disparities between the trained and encountered domains post-deployment [81,126]. Therefore, we suggest evaluating performance not only within the in-distribution (ID) domain (*i.e.*, the seen domain) but also across the out-of-distribution (OOD) domain (*i.e.*, the unseen domain).

To this end, encompassing the integration of generated data within the online CL framework, we aim to address the following specific research questions, thereby succinctly summarizing our core contributions.

1. *Is it possible for generated data to substitute manually annotated (MA) or web-crawled data in continual learning environments?* To demonstrate the effectiveness of generated data, we compared the performance of **G-NoCL** against the training with web-scraped or MA data. In our evaluation, we assess their performance not only within the in-distribution (ID) data but also across out-of-distribution (OOD) domains in online CL, using domain generalization benchmarks. *E.g.*, employing **DISCOBER** results in a 9% and 10% improvement in A_{AUC} on the PACS [143] OOD domain compared to the use of MA and web-scraped data for training, respectively.
2. *How to ensure high-quality and diverse generated images?* Within the **G-NoCL** framework, we incorporate a prompt refinement module ψ that leverages Language Models (LLMs) to generate a diverse array of fine-grained prompts. These prompts are subsequently employed for data generation in diverse settings and contexts. We illustrate the advantages of this approach by contrasting it with the use of a single base prompt for the entire volume of data generation across online continual learning benchmarks.
3. *What is the most effective approach for ensembling sampled data from various generators?* We introduce a novel ensembling technique guided by data complexity, denoted as **DISCOBER**. This technique assesses the difficulty of samples for each concept generated by individual generators, determining appropriate weights for their contributions to the ensemble. Our investigation yields two notable findings on sample hardness and previously unexplored aspects of generators.
 - Varying generators generate samples of distinct hardness even when presented with identical prompts for a fixed concept.
 - Leveraging concept-wise harder generated samples, determined by the relative Mahalanobis distance (RMD) score [30], yields superior performance in both the ID and the OOD domains.

2 Related Work

Continual learning methods and setups. To prevent catastrophic forgetting, various continual learning methods have been proposed and can be categorized as follows: regularization-based [2, 63, 70, 137], architecture-based [28, 72, 135, 142], and replay-based methods [10, 47, 65, 100, 124, 134]. However, they assume that the incoming stream data are well-curated annotated data.

For continual learning setup, many recent works propose realistic CL scenarios, such as blurry [10, 95], i-blurry [65], continuous [66, 109, 129], and noisy [11, 60] setups. However, they only focus on the realistic data distribution of the stream data, rather than the acquisition of data for a new category, for which the model needs to be learned.

A recent work [94] proposes the use of web data for continual learning, due to the high annotation cost of manually annotated data and the difficulty in acquiring real-time data for the category the model needs to learn. However, Web data have several limitations, including privacy concerns, usage restrictions, and inherent noise, as highlighted in Fig. 1. Please refer to the supplementary material for more comparison between web data and generated data.

Domain generalization. In contrast to domain adaptation, which aims to alleviate domain shift between target domains and a source domain using data from the target domain, domain generalization focuses on improving the generalizability of the model in entirely new target domains [127]. Although domain-incremental learning methods [62, 90, 102, 128] have been proposed to adapt to new domains and achieve high performance, they often involve long periods of adaptation [75].

Since long periods of adaptation are not suitable for scenarios with sudden domain shifts [75], such as autonomous driving, [113] focus on improving the generalization performance of the unseen domain with a class-incremental setup. However, they assume the use of well-curated annotated data for new classes from various domains to enhance domain generalization abilities. Meanwhile, in the real world, there are limitations in obtaining high-quality real-time data when the concept to be learned is given.

Learning from models. With the accessibility of robust generative models [13, 34, 43, 51, 52, 54–56, 93, 99, 101, 120, 141], several recent studies have investigated the potential of leveraging synthetic data for training purposes [6, 37, 68, 79, 80, 122, 123, 140]. In particular, [122] recently showcased the positive influence of employing diffusion model-generated datasets on ImageNet [32] scale for training.

Leveraging Large Language Models (LLMs) like ChatGPT [17] for CLIP [97]-based training significantly improves performance [122], suggesting generative models improve model training workflows. [140] introduces a framework to augment small datasets through conditional guided data generation using image-

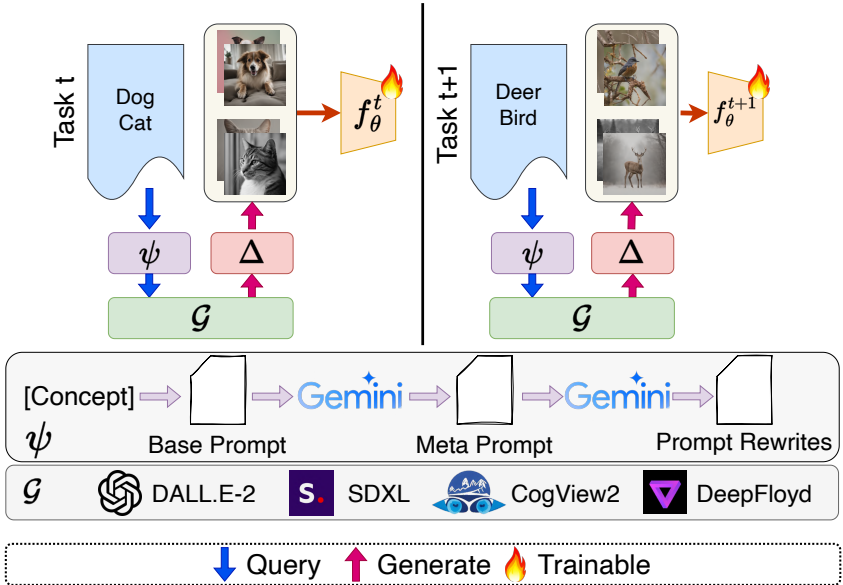


Fig. 2: G-NoCL framework: In an online CL setting, the learner f_θ receives new concepts which is passed through a prompt refiner module ψ to obtain fine-grained prompts. These prompts are subsequently used to generate data from the set of generators \mathcal{G} . The data generated by each generator are ensembled through ensembler Δ , and they are used for training the model f_θ .

generative models, yet the focus remains on supervised learning, overlooking exploration in a sequential training regime where distribution shift is common.

3 Approach

In contrast to previous works that assumed the abundance of well-curated annotated data, we explore the problem setup of online continual learning in which only new concepts are streamed to the learner f_θ without any data. We aim to address the absence of data by proposing a Generative Name only Continual Learning (**G-NoCL**) framework. The G-NoCL framework is composed of four integral components: (i) the Prompt Refiner Module ψ (Sec. 3.1), (ii) a set of Generators \mathcal{G} (Sec. 3.2), (iii) an Ensembler represented by Δ (Sec. 3.3), and (iv) the learner f_θ .

When a new concept is introduced, for which f_θ needs to be learned, a generator $g \in \mathcal{G}$ generates images related to the given concept. However, generative models have limitations in terms of the finite diversity of their output [76, 105]. Therefore, we try to maximize the output diversity of the generative model through the Prompt Refiner Module ψ . Furthermore, to enhance the diversity of generated images, we employ an ensemble approach by combining the outputs of a set of generators \mathcal{G} through a complexity-aware ensembler Δ .

When images are generated, they are promptly streamed in real-time to the learner f_θ . Simultaneously, a finite episodic memory is maintained to replay previously encountered data. One thing to note here is that, unlike real data, such as web-scraped data, storing samples in episodic memory is free from data privacy issues. While it is possible to generate data for past concepts in real-time without using episodic memory, we use it for efficiency, as it allows for reducing computational costs without privacy concerns.

*The design of the **G-NoCL** framework serves as a blueprint for category names only continual learners integrated with generators. Note that with advances in generative models and large language models (LLMs), improved models may emerge, potentially leading to the replacement of the prompt refiner module ψ and a set of generators \mathcal{G} with superior models.*

3.1 Prompt Refiner Module ψ

Given new concepts, we pass them through the prompt refiner module ψ . The pipeline ψ , as indicated in Fig. 2, initially takes the new concept as input and then constructs the base prompt. For the base prompt, we use the template: "*This is an image of the [concept]*", following [110, 112]. Although this base prompt can serve as input to the generators \mathcal{G} , generating a large number of images using the same prompt may result in limited diversity in terms of style, texture, and background elements in the generated images. So, we feed the base prompt into a language model (LLM), named Gemini [121], to generate diverse prompts, taking advantage of the in-context learning capability inherent in LLMs [17, 122]. As we rewrite those prompts in various ways to generate a more diverse set of prompts, we name them *meta prompts*.

For prompt diversification, first, we generate 10 meta-prompts based on different variations of style, background, and tone. For example, within the style category, one of the meta-prompts that we obtained was: "*A minimalist image of [concept] using clean lines and muted colors*". After obtaining the meta-prompts, we prompt Gemini [121] again to rewrite each of the meta-prompts in four different ways, thus creating a total set of 50 prompts. An example prompt-rewrite for the prompt provided above was "*Minimalist composition of [concept] with clean lines and a subdued color palette*". Note that we use the rewritten prompt without any selection and do not include domain-specific information in the prompt. Through empirical investigation, we verify that employing a two-stage prompt rewriting approach (*i.e.*, generating meta-prompts and subsequently rewriting with meta-prompts) yields greater prompt diversity compared to a single-stage prompt rewriting strategy (*i.e.*, rewriting solely with the base prompt). Please refer to the supplementary material for empirical validation and further details on the meta-prompts and prompts used in the proposed **G-NoCL** framework.

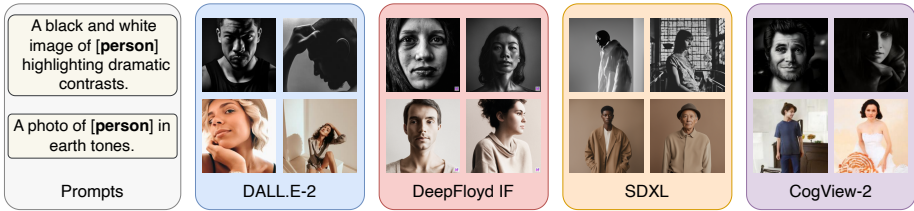


Fig. 3: Examples of PACS [143] generated samples from various generators using two of the prompt rewrites. Illustrations from the concept "Person" are showcased.

3.2 Generators \mathcal{G}

Using the prompt refiner module ψ , we increase the diversity of generated samples by a single model through the use of a range of diversified prompts, denoted as intra-diversity. Additionally, we seek to amplify the inter-diversity, the diversity between images generated by generators, by incorporating various text-to-image (T2I) generative models. Concretely, we establish a set of generators \mathcal{G} predominantly based on four distinct T2I generators: (i) Stable Diffusion XL [93], (ii) DALL.E-2 [13], (iii) CogView2 [34], and (iv) DeepFloyd IF⁶. As illustrated in Figure 3, different generators produce varied samples when prompted with identical prompts conditioned on the same concept.

3.3 Ensembler Δ

We increase the inter-diversity of generated images by using various T2I models together. Here, a question arises: *When ensembling images generated by different T2I models, which images should be included?* One of the naive yet intuitive ensemble methods is to mix images generated by each generator with equal weights. However, considering the potential existence of similar images among those generated by each generative model, it is better to mix them in a way that minimizes overlap rather than to ensemble them with the same ratio to increase inter-diversity.

To minimize overlap between generated images in the ensemble set, we focus on ensembling samples positioned far from the class prototype in the feature space, indicating those that have minimized overlap area with common images, thus challenging to classify, rather than close to the prototype, which are close to common images, thus easily identifiable. To identify such samples, we use the relative Mahalanobis distance (RMD) [30] score, which measures the difficulty in classifying a sample into a corresponding class by comparing the distance from the class prototype with the distance from the global prototype. The RMD score for a sample (x_i, y_i) is given by the following:

$$\text{RMD}(x_i, y_i) = \mathcal{M}(x_i, y_i) - \mathcal{M}_{\text{agn}}(x_i), \quad (1)$$

⁶<https://github.com/deep-floyd/IF>

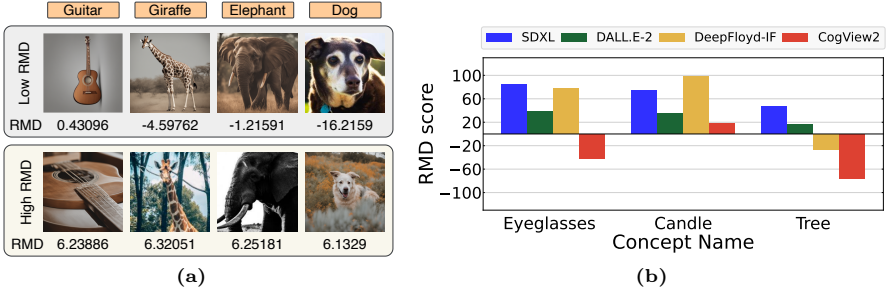


Fig. 4: (a) - Examples of samples with a high RMD score and a low RMD score, (b)- Concept-wise RMD score distributions for generated images by each generative model

where $\mathcal{M}(x_i, y_i)$ refers to the Mahalanobis distance [69] between a sample x_i and its class prototype, while $\mathcal{M}_{\text{agn}}(x_i)$ refers to the distance to the global prototype. The class prototype is obtained from the average features within a class, calculated using a frozen CLIP [97] image encoder, representing its most representative features. On the contrary, the global prototype is computed from the average features across all classes.

If the distance from the class prototype is close and the distance from the global prototype is far, leading to a low RMD score, the sample can be considered to be easy to classify into the ground truth class. Conversely, if the distance from the class prototype is far and close to the global prototype, resulting in a high RMD score, it is more likely to be classified not only as the ground truth class but also as another class, *i.e.*, the sample is difficult to classify. We show samples with low RMD scores and samples with high RMD scores in Fig. 4-(a).

By using the RMD score, we ensemble images that are difficult to classify, which are expected to exhibit a widespread dispersion from the class prototype. However, in the coreset, which is a representative subset of an entire dataset [4], it is necessary to include not only samples near the decision boundary, but also class-representative samples [10, 46].

Therefore, we use a probabilistic approach to ensemble selection, rather than just selecting images with the k -highest RMD scores. Since the diversity of generated images varies across generators for each individual class, as shown in Fig. 4-(b), we calculate a class-specific selection probability for each generator $g \in \mathcal{G}$, denoted as $p_{g|c}$ as follows:

$$p_{g|c} = \frac{e^{\overline{\text{RMD}}_{g|c}/T}}{\sum_{h \in \mathcal{G}} e^{\overline{\text{RMD}}_{h|c}/T}}, \quad (2)$$

where $\overline{\text{RMD}}_{g|c}$ is the average RMD score of the samples generated by the generator g for class c and T refers to the temperature. By adjusting model selection based on class-specific RMD scores, we enhance the diversity of the ensemble, ensuring that the ensemble includes samples that are difficult to classify.

We substantiate our hypothesis through empirical validation in a comparative study using various RMD-based ensembles, as shown in Table 1. The table

Table 1: Comparison of ensemble methods in PACS [143], using DER [18] for all ensemble methods. The proposed ensemble method outperforms other ensemble methods.

Ensemble Method Δ	ID		OOD	
	$A_{AUC} \uparrow$	$A_{last} \uparrow$	$A_{AUC} \uparrow$	$A_{last} \uparrow$
None (Baseline)	47.34±2.64	44.64±3.08	31.33±1.71	25.36±1.31
Equal weight ensemble	43.39±2.01	36.32±2.76	29.77±1.74	21.47±1.73
k -highest RMD ensemble	50.13±1.99	41.60±3.79	31.28±1.23	26.66±1.46
k -lowest RMD ensemble	31.16±0.87	21.60±2.66	25.45±1.56	11.95±1.33
Inverse Prob	40.48±1.72	23.74±0.97	27.98±0.91	20.13±1.37
DISCOBER (Ours)	50.22±2.41	45.10±1.69	32.77±1.62	28.78±1.49

reveals that DISCOBER significantly outperforms others in both In-Distribution (ID) and Out-of-Distribution (OOD) evaluations. Furthermore, with the exception of **DISCOBER**, all ensemble methods even exhibit a decrease in performance compared to the scenario where no ensembling⁷ is applied. The k -highest RMD ensemble, which excludes easy samples, leads to insufficient learning in the class-representative region, while the k -lowest RMD concentrates solely on easy samples, resulting in limited diversity. Inverse DISCOBER employs the inverse of the probabilities utilized in DISCOBER. Similar to the k -lowest RMD ensemble, it tends to prioritize easy samples, resulting in limited diversity and a decrease in performance.

Note that in online CL, where data arrive in a streaming manner, we continuously update class and global prototypes using a simple moving average and a simple moving variance [5]. For more details on the calculation of the RMD score in the online CL setup, please refer to the supplementary material.

4 Experiments

4.1 Baselines

To investigate the effectiveness of using generative models in the name-only CL setup, we performed experiments using various CL methods, and these methods can be broadly categorized into three categories: Replay-based method (ER [100], DER [18], ASER [111], MIR [3], and X-DER [16]), Regularization-based method (LiDER [15]), and Architecture-based method (MEMO [142]). For more details about the baselines, please refer to the supplementary material.

4.2 Experimental Setup

Datasets. To measure domain generalization performance, we used widely used domain generalization benchmarks: PACS [143] and DomainNet [84]. For each benchmark, data from one domain were used as in-distribution (ID) data, while

⁷No *ensembling* denotes the usage of images generated exclusively through SDXL [93] when prompted with prompt rewrites.

Table 2: Split of in-distribution (ID) domain and out-of-distribution (OOD) domain for each domain generalization benchmark.

Dataset	ID domain	OOD domain
PACS [143]	Photo	Art, Cartoon, Sketch
DomainNet [84]	Real	Clipart, Painting, Sketch
CIFAR-10-W [118]	-	CIFAR-10-W [118]
CCT [12]	10 locations	10 other locations

data from the other domain were used as out-of-distribution (OOD) data. The performance of the in-distribution (ID) domain was evaluated using the test set of the domain used for training, while the OOD performance was evaluated using data from the remaining domains (*i.e.*, domains not used for training).

We also used CIFAR-10-W [118] and CCT [12] to evaluate the performance of domain generalization. CIFAR-10-W is a dataset collected by scraping data from the Web, covering the same classes as the well-known CIFAR-10 dataset [67], and is composed of instances from cartoon and non-cartoon domains. Since it only contains data on the OOD domains, we evaluated only the performance of the out-of-distribution (OOD) domain. Note that CIFAR-10-W is a web-scraped dataset, *i.e.*, the domain of CIFAR-10-W and the web-scraped data are the same, thus we excluded the comparison with the web-scraped data in CIFAR-10-W experiments. CCT [12] is a subsampled dataset from Terra Incognita [12], a collection that captures images of animals in various fixed locations. The CCT dataset comprises data collected from a total of 20 locations.

For more details on the experiment setup, please refer to the supplementary material. We summarize the ID and OOD domain for each dataset in Tab. 2.

Metrics. We addressed a name-only online Continual Learning (CL) scenario where, upon presenting a given concept for learning, the model is trained using the generated data streamed in real time. In such an online CL setup, the model is used for inference at every moment rather than the predefined time point (*e.g.*, end of the task) [9, 20, 65, 92]. Therefore, to measure inference performance at any time, we evaluated the model at regular intervals during a specified evaluation period and then calculated the area under the accuracy curve, denoted A_{AUC} [20, 65, 66]. Furthermore, we used A_{last} to evaluate the performance of the model at the end of the training. Note that for testing, we use the test set for seen categories up to that point in time.

Implementation Details. We used ResNet-18 [48] and Vision Transformer (ViT) [35] as network architectures for all datasets. Due to the large number of parameters in ViT, training it from scratch in an online setup resulted in lower performance. Therefore, we used the weights of a model pre-trained on ImageNet-1K [103] as initial weights for ViT. For data augmentation, we consistently applied RandAugment [29] across all datasets and CL methods.

Following [59, 65, 66], we conduct batch training for each incoming sample. Specifically, for PACS, CCT, CIFAR-10-W, and DomainNet, the number

Table 3: In distribution (ID) domain and out-of-distribution (OOD) domain accuracy of CL methods when the names of PACS and DomainNet data are given incrementally. We use ResNet-18 as the backbone architecture. We followed the ID and OOD domains as described in the Tab. 2. As detailed in Sec. 3.1, we use "An image of [concept name]" as our base prompt. The term Gen. Ensemble denotes the generator ensemble, which encompasses the Diversified Prompt, *i.e.*, the result of Gen. Ensemble corresponds to the result of DISCOBER.

Method	Training Data	PACS				DomainNet			
		ID		OOD		ID		OOD	
		$A_{AUC} \uparrow$	$A_{I_{inst}} \uparrow$	$A_{AUC} \uparrow$	$A_{I_{inst}} \uparrow$	$A_{AUC} \uparrow$	$A_{I_{inst}} \uparrow$	$A_{AUC} \uparrow$	$A_{I_{inst}} \uparrow$
ER [100]	Web-scraped	53.08±2.73	50.91±2.57	29.01±2.17	24.70±0.83	31.98±0.38	23.29±0.22	9.97±0.23	6.97±0.13
	Base Prompt	46.33±1.75	45.34±3.60	27.96±1.69	20.47±1.39	25.13±0.38	21.38±0.71	7.28±0.15	5.29±0.13
	(+) Diversified Prompt	47.95±2.20	45.58±3.00	34.11±1.33	27.13±1.69	25.23±0.31	20.72±0.35	9.15±0.26	7.35±0.04
	(+) Gen. Ensemble	53.83±2.96	51.68±2.68	35.69±1.62	30.09±1.42	28.52±0.07	24.02±0.86	11.42±0.04	9.67±0.47
	Manually Annotated	70.21±3.71	72.11±1.57	28.53±1.81	22.08±1.31	48.56±0.23	40.22±0.55	12.68±0.10	10.19±0.18
ER-MIR [3]	Web-scraped	47.45±4.47	44.57±5.26	27.97±2.20	18.17±1.55	32.39±0.31	23.36±0.32	10.25±0.23	7.26±0.07
	Base Prompt	49.34±2.11	46.71±0.83	28.24±1.56	21.00±2.16	24.81±0.43	21.17±0.32	7.23±0.22	5.73±0.15
	(+) Diversified Prompt	50.46±2.18	49.62±3.43	34.36±1.82	28.02±1.16	24.82±0.20	20.56±0.35	9.10±0.20	7.51±0.15
	(+) Gen. Ensemble	54.28±3.84	55.31±1.05	37.42±1.80	33.90±0.93	28.36±0.13	23.74±0.37	11.43±0.13	9.59±0.19
	Manually Annotated	68.15±5.06	70.98±1.98	28.78±2.26	21.14±1.04	49.20±0.10	40.54±0.46	12.96±0.03	10.33±0.25
DER++ [18]	Web-scraped	48.39±3.17	36.50±4.24	26.89±1.86	18.88±1.00	32.09±0.36	22.37±0.42	9.92±0.20	6.42±0.04
	Base Prompt	41.47±2.26	39.41±2.90	27.74±1.41	18.82±1.57	26.64±0.39	22.04±0.47	7.91±0.24	5.85±0.05
	(+) Diversified Prompt	47.34±2.64	41.60±4.08	32.33±1.71	25.36±1.31	25.61±0.36	20.06±0.38	9.40±0.13	7.20±0.17
	(+) Gen. Ensemble	49.02±2.41	45.10±1.69	33.07±1.62	28.78±1.49	29.67±0.06	23.37±0.38	11.89±0.02	9.41±0.16
	Manually Annotated	63.90±5.04	61.19±2.92	27.49±1.77	19.75±1.58	43.35±0.33	39.40±0.20	12.62±0.13	9.27±0.18
ASER [111]	Web-scraped	49.12±3.32	42.49±4.06	27.50±1.92	19.04±1.48	33.80±0.38	23.09±0.84	9.80±0.51	6.43±0.69
	Base Prompt	40.35±1.25	38.04±2.79	26.64±1.28	18.06±0.80	25.42±0.24	22.93±0.19	7.71±0.64	5.51±0.76
	(+) Diversified Prompt	48.28±0.67	45.40±2.95	33.76±1.20	25.48±1.94	20.94±0.26	20.93±0.31	9.87±0.02	5.64±0.44
	(+) Gen. Ensemble	48.38±1.95	47.24±2.07	35.07±1.46	31.58±2.09	32.01±0.85	24.28±0.70	11.56±0.62	8.25±0.98
	Manually Annotated	68.00±4.95	70.33±2.58	26.81±1.72	19.21±1.16	48.92±0.43	40.93±0.12	10.51±1.27	6.43±0.12
MEMO [142]	Web-scraped	49.27±2.52	39.88±4.93	28.00±1.53	19.19±1.36	30.17±0.25	21.40±0.24	9.29±0.27	6.28±0.03
	Base Prompt	43.67±0.90	39.76±4.72	27.22±1.09	17.00±0.67	23.54±0.32	19.45±0.22	6.82±0.16	4.98±0.05
	(+) Diversified Prompt	48.80±1.69	46.59±2.50	32.21±1.55	24.56±0.47	23.59±0.22	19.30±0.30	8.63±0.11	6.83±0.11
	(+) Gen. Ensemble	50.20±2.37	48.72±0.91	33.50±1.36	29.43±2.79	26.88±0.35	21.67±0.20	10.61±0.13	8.58±0.19
	Manually Annotated	67.37±4.67	66.94±2.26	27.73±1.59	20.63±0.71	47.04±0.43	38.25±0.45	11.77±0.20	8.99±0.26
X-DER [16]	Web-scraped	50.44±2.93	41.96±2.11	27.57±1.78	20.73±0.16	31.68±0.21	23.00±0.95	10.93±0.44	8.54±0.10
	Base Prompt	44.78±2.77	46.59±2.62	29.86±1.63	22.86±0.99	27.41±0.23	24.11±0.85	7.91±0.65	6.65±0.12
	(+) Diversified Prompt	49.68±2.97	46.94±3.53	33.61±2.07	24.74±2.70	26.72±0.75	21.71±0.43	9.28±0.86	7.65±0.39
	(+) Gen. Ensemble	50.52±1.57	48.19±2.47	33.69±1.36	26.73±0.54	32.14±0.52	25.48±0.16	12.39±0.74	10.04±0.54
	Manually Annotated	66.19±4.78	68.49±1.85	28.61±1.92	20.54±0.81	50.35±0.20	42.41±0.14	12.99±0.29	10.68±0.83
LiDER [15]	Web-scraped	51.07±3.06	44.69±2.22	27.95±1.60	22.16±1.22	30.95±0.34	23.55±0.28	9.93±0.20	7.25±0.08
	Base Prompt	45.73±2.65	43.26±4.86	29.24±1.30	22.12±1.07	24.27±0.20	21.29±0.45	7.05±0.08	5.55±0.06
	(+) Diversified Prompt	51.74±2.48	51.40±2.79	34.04±1.90	27.10±1.41	24.55±0.10	20.78±0.39	9.05±0.16	7.56±0.14
	(+) Gen. Ensemble	52.46±3.11	52.35±3.26	36.18±1.44	30.94±1.24	30.09±0.41	24.04±0.32	11.42±0.34	9.26±0.29
	Manually Annotated	66.31±5.69	66.59±2.60	29.11±2.19	21.21±1.03	47.75±0.16	40.06±0.35	12.34±0.09	10.06±0.08

of batch iterations per incoming sample is set to 2, 2, 2, and 3, respectively, with batch sizes of 16, 16, 16, and 64. Episodic memory sizes are configured as 200, 400, 1000, and 8000 for PACS, CCT, CIFAR-10-W, and DomainNet, respectively. To ensure a fair comparison among manually annotated data, generated data, and web-scraped data, we used an equal number of samples in all experiments. Regarding the web-scraped data, we obtained 20% more samples than necessary for batch training with the aim of filtering out noisy data. To achieve this, we utilized pre-trained CLIP [97] for filtering, which excludes the most noisy bottom samples, resulting in a cleaned subset used for training, following [107].

In all experiments, we run five different random seeds and report the average and standard error mean. For the class-incremental setup, we adopt a disjoint configuration, where tasks do not share classes [91]. We employ the Gem-

ini model [121], a Large Language Model, to generate diverse meta-prompts. On manual inspection, Gemini exhibits superior performance in producing well-structured meta-prompts compared to ChatGPT [17].

4.3 Results

To assess whether our proposed method works well in a setup where only class names are provided without data, we compare it with the scraped data from the Web. Additionally, we compare the performance when manually annotated data are provided as an ideal case. We summarize the results not only in the ID domain but also in the OOD domain in Tab. 3, Tab. 4, and Tab. 5.

In-distribution (ID) domain evaluation uses the test set of manually annotated (MA) data. Hence, we anticipate that the model trained using manually annotated (MA) data will establish an upper performance bound, showcasing superior results in comparison. However, interestingly, in the out-of-distribution (OOD) domain of PACS, DISCOBER outperforms not only MA data but also web-scraped data. We believe that we achieve better generalization performance by generating a more diverse set of images through a diversified set of prompts and an ensemble of generators. One thing to note here is that DomainNet is a benchmark created through web scraping, resulting in a domain overlap with web data. Despite this, DISCOBER outperforms the web-scraped data in DomainNet.

CCT is a domain-specific benchmark captured by fixing cameras at various locations in the wild, including photos taken at night or obscured by natural elements such as trees or rocks. Therefore, although photos taken at different locations are categorized as OOD in CCT, OOD data include a substantial number of images resembling the ID domain, in contrast to web-scraped or generated data. Due to these domain-specific characteristics, models trained on MA data in CCT exhibit superior performance across both ID and OOD domains compared to models trained on web-scraped or generated data. When evaluating the performance of models trained on web-scraped data against data generated using DISCOBER in CCT, DISCOBER demonstrates superior performance in both ID and OOD domains.

In summary, we explore the G-NoCL setup where only the concept names that learners need to learn are provided. When exclusively trained on images generated using DISCOBER, without relying on any human-annotated MA data, we achieved the best performance in the OOD domains of all benchmarks (*i.e.*,

Table 4: Comparison of Manually Annotated (MA) data and DISCOBER on CIFAR-10-W. We use ResNet-18 as the backbone.

Method	Training Data	$A_{AUC} \uparrow$	$A_{last} \uparrow$
ER	DISCOBER	60.93±3.92	48.20±0.27
	MA	48.97±0.56	31.27±2.31
ER-MIR	DISCOBER	58.19±0.86	46.01±0.34
	MA	44.77±0.86	35.01±2.50
DER++	DISCOBER	53.88±1.22	39.53±1.42
	MA	45.25±0.07	28.75±1.44
ASER	DISCOBER	54.34±0.66	41.88±1.00
	MA	50.00±0.59	34.86±1.17
MEMO	DISCOBER	53.59±0.67	41.69±0.67
	MA	45.40±0.56	30.97±2.13
X-DER	DISCOBER	57.56±0.75	45.97±0.17
	MA	47.14±0.82	33.41±1.34
LiDER	DISCOBER	57.13±0.29	45.41±2.58
	MA	46.97±0.42	28.79±4.27

Table 5: In distribution (ID) domain and out-of-distribution (OOD) domain accuracy of CL methods when the names of PACS and CCT data are given incrementally. We use ViT [104] as the backbone architecture. We followed the ID and OOD domains as described in the Tab. 2. MA denotes manual annotations.

Method	Training Data	PACS				CCT			
		ID		OOD		ID		OOD	
		$A_{AUC} \uparrow$	$A_{last} \uparrow$	$A_{AUC} \uparrow$	$A_{last} \uparrow$	$A_{AUC} \uparrow$	$A_{last} \uparrow$	$A_{AUC} \uparrow$	$A_{last} \uparrow$
ER [100]	Web-scraped	47.12±4.67	30.51±5.98	29.78±1.90	15.71±1.94	24.98±1.02	11.00±0.90	21.71±0.75	9.93±0.78
	DISCOBER	55.25±4.11	48.84±3.95	33.24±1.62	23.14±1.21	25.50±0.99	12.03±0.81	25.16±0.56	14.13±0.95
	Manually Annotated	72.93±5.29	70.51±1.75	30.68±1.95	20.85±0.84	52.20±2.52	34.07±3.41	42.29±1.55	22.10±2.13
ER-MIR [3]	Web-scraped	48.78±5.96	40.95±5.92	28.71±2.24	20.03±3.24	23.07±3.31	12.37±2.78	22.64±2.43	12.20±4.23
	DISCOBER	50.74±4.09	51.51±1.83	31.84±1.93	25.17±1.05	23.72±0.18	12.59±0.65	24.82±0.34	14.01±4.83
	Manually Annotated	68.21±6.44	73.29±1.90	28.69±1.96	23.03±0.85	37.75±1.36	18.99±1.43	33.38±0.70	15.31±1.27
DER++ [18]	Web-scraped	53.61±3.39	45.71±4.20	27.66±1.46	18.75±1.63	23.19±0.51	9.17±1.11	22.17±0.60	8.93±0.66
	DISCOBER	50.44±4.32	43.96±3.32	30.30±1.81	20.91±0.86	25.24±1.28	10.63±0.85	24.39±0.92	10.17±0.73
	Manually Annotated	64.81±6.75	61.36±2.37	28.94±2.03	19.95±1.64	44.05±2.67	19.50±2.78	38.02±1.18	17.10±2.21
ASER [111]	Web-scraped	56.32±5.10	49.55±4.53	30.67±2.58	21.82±2.04	25.48±1.05	12.84±1.40	22.33±0.85	12.23±0.99
	DISCOBER	56.06±4.60	52.04±3.85	33.99±2.02	25.81±0.92	26.15±1.74	13.97±1.04	24.85±1.13	12.73±1.36
	Manually Annotated	77.83±7.77	76.48±9.23	43.37±4.28	35.87±7.47	54.28±1.71	47.67±1.85	45.07±1.56	28.07±0.72

PACS, CCT, CIFAR-10-W, and DomainNet) with which we experimented. Additionally, compared to web-scraped data, our approach outperforms ID domain accuracy in the majority of benchmarks, excluding some ID domains, and consistently outperforms OOD domain accuracy across all benchmarks we used.

4.4 Ablation Study

We conduct an ablation study on two components of DISCOBER, namely the diversified prompt and generator ensemble, and summarize the results in Tab. 3. Our observations indicate that both the diversified prompt and generator ensemble play a significant role in enhancing not only the ID domain performance but also the OOD domain performance.

4.5 Scaling behavior

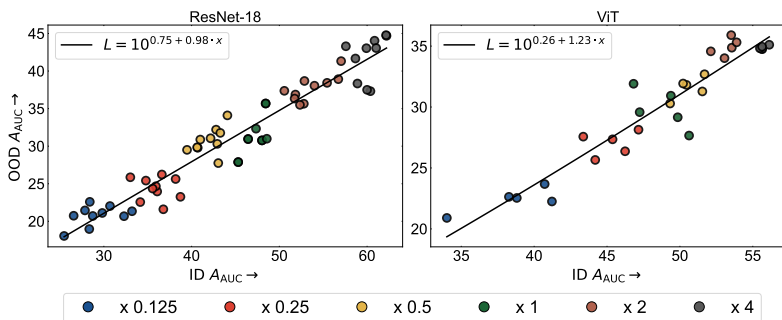


Fig. 5: Ensemble scaling behavior of (a) ResNet-18 [48] and (b) ViT [35] for ID A_{AUC} vs. OOD A_{AUC} on the PACS dataset [143] using ER [100]. (x 1) denotes the ensemble volume in primary experiments, the default data budget.

Recent scaling law studies [49, 50] offer predictive insight into model performance by scaling computation, data, and model capacity. Despite the limited exploration of scaling in continual learning settings [98], and particularly with synthetic data [36] being confined to static frameworks, our empirical analysis in Fig. 5 delves into scaling dynamics with varying generated data proportions for training online continual learners.

For ResNet-18 [48] and ViT [35], we observe a consistent linear improvement trend in both ID and OOD A_{AUC} as the volume of generated data increases in the PACS [143] dataset. This scaling behavior underscores the positive correlation between performance improvement and larger, optimally curated generated data ensembles in online continual learning, reinforcing the rationale for the use of generators in the absence of annotated data.

4.6 Justification for the Use of RMD Score

















	Dog		Horse		Guitar		Elephant	
High RMD, High RS								
	RMD: 4.4 RS: 49.17	RMD: 4.7 RS: 41.48	RMD: 4.9 RS: 41.14	RMD: 5.2 RS: 40.39	RMD: 4.3 RS: 41.55	RMD: 4.6 RS: 37.09	RMD: 4.4 RS: 37.71	RMD: 4.9 RS: 41.99
Low RMD, Low RS								
	RMD: 0.3 RS: 28.54	RMD: 1.5 RS: 30.91	RMD: 1.4 RS: 29.82	RMD: 1.7 RS: 31.72	RMD: 0.6 RS: 26.9	RMD: 0.5 RS: 24.67	RMD: 0.4 RS: 29.16	RMD: 2.1 RS: 26.12

Fig. 6: Examples of samples with high RMD scores and high Rarity scores (RS), as well as instances with low RMD scores and low Rarity scores (RS). The average RMD scores for Dog, Horse, Guitar, and Elephant are 2.91, 3.03, 2.43, and 3.25, respectively, while the corresponding average Rarity scores (RS) are 33.59, 33.58, 33.57, and 33.18.

Many recent works endeavor to qualitatively assess the diversity [45, 61, 83], complexity [53], aesthetics [57, 116], and realism [23, 26, 27] of the generated images. In our work, we use the relative Mahalanobis distance (RMD) score [30], to evaluate the complexity of the generated samples. However, there is still an important question about why we have chosen to prioritize RMD over other metrics and how well RMD aligns with existing complexity metrics.

The reason for selecting RMD as a complexity metric is its independence from the need for real samples in its calculation, while other diversity metric, such as the Rarity Score [45] and the TopP&R [61] requires *real* samples, data that has not been generated, to measure diversity. Given that our proposed framework, G-NoCL, operates exclusively with *concept* inputs rather than *real* data, we cannot utilize *real* data to measure diversity.

As we can see in Fig. 6, samples that have high RMD scores have high Rarity scores. Note that the Rarity score uses real samples to calculate the

complexity of the generated images. This result shows the ability of the RMD score to effectively measure complexity even in the absence of real samples. Consequently, it advocates for the adoption of our proposed G-NoCL framework, which operates under the assumption that manually annotated data (*i.e.*, real data) are unavailable.

5 Conclusion

Online continual learning represents a practical and real-world-aligned learning paradigm. However, assumptions regarding the availability of high-quality, diverse and annotated data in such scenarios lack a solid foundation. In addressing the challenges associated with training on web-crawled and manually annotated data, we introduce a unified name-only online continual learning framework that integrates generators with the continual learner, termed "Generative Name only Continual Learning" (**G-NoCL**).

Within the G-NoCL framework, we propose an inaugural method for prompt diversification (ψ) and sample complexity-guided ensembling (Δ), denoted as **DISCOBER**. Extensive experimental evaluations demonstrate the performance improvements achieved by DISCOBER within the G-NoCL framework, showcasing its effectiveness in both in-distribution (ID) and out-of-distribution (OOD) settings compared to webly-supervised and manually annotated approaches.

Limitations and future work. While DISCOBER provides a foundational strategy for optimal generator ensembling, we acknowledge limitations arising from the use of curated prompt rewrites without incorporating feedback from the continual learner. In addition, we acknowledge limitations associated with the fact that the generative model cannot produce high-quality images in all domains without fine-tuning.

In future endeavors, our aim is to expand the G-NoCL framework into multi-concept settings, leveraging and enhancing the compositional generation capabilities of T2I models. This extension encompasses broadening the proposed framework to dense prediction tasks such as semantic segmentation and object detection, and tasks in other modalities such as code generation.

References

1. Agun, H.V.: Webcollectives: A light regular expression based web content extractor in java. In: SoftwareX. vol. 24, p. 101569. Elsevier (2023) 2
2. Aljundi, R., Babiloni, F., Elhoseiny, M., Rohrbach, M., Tuytelaars, T.: Memory aware synapses: Learning what (not) to forget. In: ECCV (2018) 4
3. Aljundi, R., Caccia, L., Belilovsky, E., Caccia, M., Lin, M., Charlin, L., Tuytelaars, T.: Online continual learning with maximally interfered retrieval. In: NeurIPS (2019) 1, 9, 11, 13, 24
4. Anonymous: Coreset selection for object detection (2023), <https://openreview.net/forum?id=Yyg3DXzaIK> 8

5. Attia, J.: Evaluating the effectiveness of common technical trading models. arXiv preprint arXiv:1907.10407 (2019) **9**
6. Azizi, S., Kornblith, S., Saharia, C., Norouzi, M., Fleet, D.J.: Synthetic data from diffusion models improves imagenet classification. arXiv preprint arXiv:2304.08466 (2023) **4**
7. Bain, M., Nagrani, A., Varol, G., Zisserman, A.: Frozen in time: A joint video and image encoder for end-to-end retrieval. In: ICCV (2021) **25**
8. Balloccu, S., Schmidová, P., Lango, M., Dušek, O.: Leak, cheat, repeat: Data contamination and evaluation malpractices in closed-source llms. arXiv preprint arXiv:2402.03927 (2024) **25**
9. Banerjee, S., Verma, V.K., Mukherjee, A., Gupta, D., Namboodiri, V.P., Rai, P.: Verse: Virtual-gradient aware streaming lifelong learning with anytime inference. arXiv preprint arXiv:2309.08227 (2023) **10**
10. Bang, J., Kim, H., Yoo, Y., Ha, J.W., Choi, J.: Rainbow memory: Continual learning with a memory of diverse samples. In: CVPR (2021) **4, 8**
11. Bang, J., Koh, H., Park, S., Song, H., Ha, J.W., Choi, J.: Online continual learning on a contaminated data stream with blurry task boundaries. In: Proceedings of the IEEE/CVF Conference on Computer Vision and Pattern Recognition. pp. 9275–9284 (2022) **4**
12. Beery, S., Van Horn, G., Perona, P.: Recognition in terra incognita. In: ECCV (2018) **10, 24, 32**
13. Betker, J., Goh, G., Jing, L., Brooks, T., Wang, J., Li, L., Ouyang, L., Zhuang, J., Lee, J., Guo, Y., et al.: Improving image generation with better captions. Computer Science. <https://cdn.openai.com/papers/dall-e-3.pdf> **2**(3), 8 (2023) **4, 7**
14. Bianchi, F., Kalluri, P., Durmus, E., Ladhak, F., Cheng, M., Nozza, D., Hashimoto, T., Jurafsky, D., Zou, J., Caliskan, A.: Easily accessible text-to-image generation amplifies demographic stereotypes at large scale. In: FAccT (2023) **2**
15. Bonicelli, L., Boschini, M., Porrello, A., Spampinato, C., Calderara, S.: On the effectiveness of lipschitz-driven rehearsal in continual learning. In: NeurIPS (2022) **9, 11, 24**
16. Boschini, M., Bonicelli, L., Buzzega, P., Porrello, A., Calderara, S.: Class-incremental continual learning into the extended der-verse. In: TPAMI. IEEE (2022) **9, 11, 24**
17. Brown, T., Mann, B., Ryder, N., Subbiah, M., Kaplan, J.D., Dhariwal, P., Neelakantan, A., Shyam, P., Sastry, G., Askell, A., et al.: Language models are few-shot learners. In: NeurIPS (2020) **4, 6, 12, 34, 35**
18. Buzzega, P., Boschini, M., Porrello, A., Abati, D., Calderara, S.: Dark experience for general continual learning: a strong, simple baseline. In: NeurIPS (2020) **9, 11, 13, 24**
19. Byeon, M., Park, B., Kim, H., Lee, S., Baek, W., Kim, S.: Coyo-700m: Image-text pair dataset. <https://github.com/kakaobrain/coyo-dataset> (2022) **25**
20. Caccia, L., Xu, J., Ott, M., Ranzato, M., Denoyer, L.: On anytime learning at macroscale. In: CoLLAs. PMLR (2022) **10**
21. Caliskan, A., Bryson, J.J., Narayanan, A.: Semantics derived automatically from language corpora contain human-like biases. *Science* **356**(6334), 183–186 (2017) **25**
22. Carvalho, T., Moniz, N., Antunes, L., Chawla, N.: Differentially-private data synthetisation for efficient re-identification risk control. arXiv preprint arXiv:2212.00484 (2022) **26**

23. Chen, M., Liu, Y., Yi, J., Xu, C., Lai, Q., Wang, H., Ho, T.Y., Xu, Q.: Evaluating text-to-image generative models: An empirical study on human image synthesis. arXiv preprint arXiv:2403.05125 (2024) [14](#)
24. Chen, Q., Xiang, C., Xue, M., Li, B., Borisov, N., Kaarfar, D., Zhu, H.: Differentially private data generative models. arXiv preprint arXiv:1812.02274 (2018) [26](#)
25. Chen, X., Navidi, T., Ermon, S., Rajagopal, R.: Distributed generation of privacy preserving data with user customization. arXiv preprint arXiv:1904.09415 (2019) [26](#)
26. Chen, Y., Akhtar, N., Haldar, N.A.H., Mian, A.: On quantifying and improving realism of images generated with diffusion. arXiv preprint arXiv:2309.14756 (2023) [14](#)
27. Chen, Z., Sun, W., Wu, H., Zhang, Z., Jia, J., Min, X., Zhai, G., Zhang, W.: Exploring the naturalness of ai-generated images. arXiv preprint arXiv:2312.05476 (2023) [14](#)
28. Cheung, B., Terekhov, A., Chen, Y., Agrawal, P., Olshausen, B.: Superposition of many models into one. In: NeurIPS (2019) [4](#)
29. Cubuk, E.D., Zoph, B., Shlens, J., Le, Q.V.: Randaugment: Practical automated data augmentation with a reduced search space. In: CVPRW (2020) [10](#)
30. Cui, P., Zhang, D., Deng, Z., Dong, Y., Zhu, J.: Learning sample difficulty from pre-trained models for reliable prediction. In: NeurIPS (2024) [3](#), [7](#), [14](#), [27](#)
31. Dekoninck, J., Müller, M.N., Baader, M., Fischer, M., Vechev, M.: Evading data contamination detection for language models is (too) easy. arXiv preprint arXiv:2402.02823 (2024) [25](#)
32. Deng, J., Dong, W., Socher, R., Li, L.J., Li, K., Fei-Fei, L.: Imagenet: A large-scale hierarchical image database. In: CVPR (2009). <https://doi.org/10.1109/CVPR.2009.5206848> [4](#)
33. Ding, K., Ma, K., Wang, S., Simoncelli, E.P.: Image quality assessment: Unifying structure and texture similarity. IEEE transactions on pattern analysis and machine intelligence **44**(5), 2567–2581 (2020) [41](#)
34. Ding, M., Zheng, W., Hong, W., Tang, J.: Cogview2: Faster and better text-to-image generation via hierarchical transformers. In: NeurIPS (2022) [4](#), [7](#)
35. Dosovitskiy, A., Brox, T.: Inverting visual representations with convolutional networks. In: CVPR (2016) [10](#), [13](#), [14](#)
36. Fan, L., Chen, K., Krishnan, D., Katabi, D., Isola, P., Tian, Y.: Scaling laws of synthetic images for model training... for now. arXiv preprint arXiv:2312.04567 (2023) [14](#)
37. Fan, L., Krishnan, D., Isola, P., Katabi, D., Tian, Y.: Improving clip training with language rewrites. In: NeurIPS (2024) [4](#)
38. Feng, F., Yang, Y., Cer, D., Arivazhagan, N., Wang, W.: Language-agnostic BERT sentence embedding. In: Muresan, S., Nakov, P., Villavicencio, A. (eds.) Proceedings of the 60th Annual Meeting of the Association for Computational Linguistics (Volume 1: Long Papers). pp. 878–891. Association for Computational Linguistics, Dublin, Ireland (May 2022). <https://doi.org/10.18653/v1/2022.acl-long.62>, <https://aclanthology.org/2022.acl-long.62> [35](#)
39. Foerderer, J.: Should we trust web-scraped data? arXiv preprint arXiv:2308.02231 (2023) [25](#)
40. Fraser, K.C., Kiritchenko, S., Nejadgholi, I.: Diversity is not a one-way street: Pilot study on ethical interventions for racial bias in text-to-image systems. In: ICCV (2023) [2](#)

41. Gao, L., Biderman, S., Black, S., Golding, L., Hoppe, T., Foster, C., Phang, J., He, H., Thite, A., Nabeshima, N., et al.: The pile: An 800gb dataset of diverse text for language modeling. arXiv preprint arXiv:2101.00027 (2020) 25
42. Ghunaim, Y., Bibi, A., Alhamoud, K., Alfarra, M., Al Kader Hammoud, H.A., Prabhu, A., Torr, P.H., Ghanem, B.: Real-time evaluation in online continual learning: A new hope. In: CVPR (2023) 24
43. Gu, J., Gao, Q., Zhai, S., Chen, B., Liu, L., Susskind, J.: Learning controllable 3d diffusion models from single-view images. arXiv preprint arXiv:2304.06700 (2023) 4
44. Günther, M., Ong, J., Mohr, I., Abdessalem, A., Abel, T., Akram, M.K., Guzman, S., Mastrapas, G., Sturua, S., Wang, B., Werk, M., Wang, N., Xiao, H.: Jina embeddings 2: 8192-token general-purpose text embeddings for long documents (2023) 35
45. Han, J., Choi, H., Choi, Y., Kim, J., Ha, J.W., Choi, J.: Rarity score: A new metric to evaluate the uncommonness of synthesized images. arXiv preprint arXiv:2206.08549 (2022) 14, 41
46. Harun, M.Y., Gallardo, J., Kanan, C.: Grasp: A rehearsal policy for efficient online continual learning. arXiv preprint arXiv:2308.13646 (2023) 8
47. Hayes, T.L., Kafle, K., Shrestha, R., Acharya, M., Kanan, C.: Remind your neural network to prevent catastrophic forgetting. In: ECCV (2020) 4
48. He, K., Zhang, X., Ren, S., Sun, J.: Deep residual learning for image recognition. In: CVPR (2016) 10, 13, 14, 32
49. Hernandez, D., Kaplan, J., Henighan, T., McCandlish, S.: Scaling laws for transfer. arXiv preprint arXiv:2102.01293 (2021) 14
50. Hoffmann, J., Borgeaud, S., Mensch, A., Buchatskaya, E., Cai, T., Rutherford, E., Casas, D.d.L., Hendricks, L.A., Welbl, J., Clark, A., et al.: Training compute-optimal large language models. arXiv preprint arXiv:2203.15556 (2022) 14
51. Huang, Q., Park, D.S., Wang, T., Denk, T.I., Ly, A., Chen, N., Zhang, Z., Zhang, Z., Yu, J., Frank, C., et al.: Noise2music: Text-conditioned music generation with diffusion models. arXiv preprint arXiv:2302.03917 (2023) 4
52. Huang, R., Huang, J., Yang, D., Ren, Y., Liu, L., Li, M., Ye, Z., Liu, J., Yin, X., Zhao, Z.: Make-an-audio: Text-to-audio generation with prompt-enhanced diffusion models. arXiv preprint arXiv:2301.12661 (2023) 4
53. Hwang, J., Lee, J., Lee, J.S.: Anomaly score: Evaluating generative models and individual generated images based on complexity and vulnerability. arXiv preprint arXiv:2312.10634 (2023) 14
54. Kang, M., Min, D., Hwang, S.J.: Any-speaker adaptive text-to-speech synthesis with diffusion models. arXiv preprint arXiv:2211.09383 (2022) 4
55. Karnewar, A., Vedaldi, A., Novotny, D., Mitra, N.J.: Holodiffusion: Training a 3d diffusion model using 2d images. In: CVPR (2023) 4
56. Khader, F., Mueller-Franzes, G., Arasteh, S.T., Han, T., Haarburger, C., Schulze-Hagen, M., Schad, P., Engelhardt, S., Baessler, B., Foersch, S., et al.: Medical diffusion–denoising diffusion probabilistic models for 3d medical image generation. arXiv preprint arXiv:2211.03364 (2022) 4
57. Khajehabdollahi, S., Martius, G., Levina, A.: Assessing aesthetics of generated abstract images using correlation structure. In: 2019 IEEE Symposium Series on Computational Intelligence (SSCI). pp. 306–313. IEEE (2019) 14
58. Khan, M., Hanna, A.: The legality of computer vision datasets. Under review (2020) 25

59. Kim, B., Seo, M., Choi, J.: Online continual learning for interactive instruction following agents. In: OpenReview (2024), <https://openreview.net/forum?id=7MOEzjugaN> 10
60. Kim, C.D., Jeong, J., Moon, S., Kim, G.: Continual learning on noisy data streams via self-purified replay. In: ICCV (2021) 4
61. Kim, P.J., Jang, Y., Kim, J., Yoo, J.: Topp&r: Robust support estimation approach for evaluating fidelity and diversity in generative models. Advances in Neural Information Processing Systems 36 (2024) 14
62. Kiran, M., Pedersoli, M., Dolz, J., Blais-Morin, L.A., Granger, E., et al.: Incremental multi-target domain adaptation for object detection with efficient domain transfer. In: PR (2022) 4
63. Kirkpatrick, J., Pascanu, R., Rabinowitz, N., Veness, J., Desjardins, G., Rusu, A.A., Milan, K., Quan, J., Ramalho, T., Grabska-Barwinska, A., et al.: Overcoming catastrophic forgetting in neural networks. In: PNAS (2017) 4
64. Kocetkov, D., Li, R., Allal, L.B., Li, J., Mou, C., Ferrandis, C.M., Jernite, Y., Mitchell, M., Hughes, S., Wolf, T., et al.: The stack: 3 tb of permissively licensed source code. arXiv preprint arXiv:2211.15533 (2022) 25
65. Koh, H., Kim, D., Ha, J.W., Choi, J.: Online continual learning on class incremental blurry task configuration with anytime inference. In: ICLR (2021) 1, 4, 10
66. Koh, H., Seo, M., Bang, J., Song, H., Hong, D., Park, S., Ha, J.W., Choi, J.: Online boundary-free continual learning by scheduled data prior. In: ICLR (2023) 4, 10
67. Krizhevsky, A., Hinton, G., et al.: Learning multiple layers of features from tiny images (2009) 10, 40, 41
68. Kumar, V., Choudhary, A., Cho, E.: Data augmentation using pre-trained transformer models. arXiv preprint arXiv:2003.02245 (2020) 4
69. Lee, K., Lee, K., Lee, H., Shin, J.: A simple unified framework for detecting out-of-distribution samples and adversarial attacks. In: NeurIPS (2018) 8
70. Lesort, T., Stoian, A., Filliat, D.: Regularization shortcomings for continual learning. arXiv preprint arXiv:1912.03049 (2019) 4
71. Li, W., Wang, L., Li, W., Agustsson, E., Van Gool, L.: Webvision database: Visual learning and understanding from web data. arXiv preprint arXiv:1708.02862 (2017) 2
72. Li, X., Zhou, Y., Wu, T., Socher, R., Xiong, C.: Learn to grow: A continual structure learning framework for overcoming catastrophic forgetting. In: ICML. PMLR (2019) 4
73. Li, Y.: An open source data contamination report for llama series models. arXiv preprint arXiv:2310.17589 (2023) 25
74. Liang, J., Wu, C., Hu, X., Gan, Z., Wang, J., Wang, L., Liu, Z., Fang, Y., Duan, N.: Nuwa-infinity: Autoregressive over autoregressive generation for infinite visual synthesis. In: NeurIPS (2022) 2
75. Liu, C., Wang, L., Lyu, L., Sun, C., Wang, X., Zhu, Q.: Deja vu: Continual model generalization for unseen domains. In: ICLR (2022) 4
76. Liu, G., Li, Y., Fei, Z., Fu, H., Luo, X., Guo, Y.: Prefix-diffusion: A lightweight diffusion model for diverse image captioning. arXiv preprint arXiv:2309.04965 (2023) 5
77. Lukas, N., Salem, A., Sim, R., Tople, S., Wutschitz, L., Zanella-Béguelin, S.: Analyzing leakage of personally identifiable information in language models. arXiv preprint arXiv:2302.00539 (2023) 26
78. Madaan, D., Yoon, J., Li, Y., Liu, Y., Hwang, S.J.: Representational continuity for unsupervised continual learning. arXiv preprint arXiv:2110.06976 (2021) 2

79. Meng, Y., Huang, J., Zhang, Y., Han, J.: Generating training data with language models: Towards zero-shot language understanding. In: *NeurIPS (2022)* [4](#)
80. Mimura, M., Ueno, S., Inaguma, H., Sakai, S., Kawahara, T.: Leveraging sequence-to-sequence speech synthesis for enhancing acoustic-to-word speech recognition. In: *SLT. IEEE (2018)* [4](#)
81. Mirza, M.J., Masana, M., Possegger, H., Bischof, H.: An efficient domain-incremental learning approach to drive in all weather conditions. In: *CVPR (2022)* [3](#)
82. Murgia, M., Harlow, M.: Who’s using your face? the ugly truth about facial recognition. *Financial Times* **19**, 1 (2019) [26](#)
83. Naeem, M.F., Oh, S.J., Uh, Y., Choi, Y., Yoo, J.: Reliable fidelity and diversity metrics for generative models. In: *International Conference on Machine Learning*. pp. 7176–7185. PMLR (2020) [14](#)
84. Neyshabur, B., Sedghi, H., Zhang, C.: What is being transferred in transfer learning? In: *NeurIPS (2020)* [2](#), [9](#), [10](#), [24](#)
85. Ni, J., Abrego, G.H., Constant, N., Ma, J., Hall, K.B., Cer, D., Yang, Y.: Sentence-t5: Scalable sentence encoders from pre-trained text-to-text models. *arXiv preprint arXiv:2108.08877* (2021) [35](#)
86. Nie, W., Vahdat, A., Anandkumar, A.: Controllable and compositional generation with latent-space energy-based models. In: *NeurIPS (2021)* [2](#)
87. Niu, L., Tang, Q., Veeraraghavan, A., Sabharwal, A.: Learning from noisy web data with category-level supervision. In: *CVPR (2018)* [2](#)
88. O’Sullivan, L.: Don’t steal data. In: *NeurIPS (2020)* [26](#)
89. Packer, B., Mitchell, M., Guajardo-Céspedes, M., Halpern, Y.: Text embeddings contain bias. here’s why that matters. (2018) [25](#)
90. Panagiotakopoulos, T., Dovesi, P.L., Härenstam-Nielsen, L., Poggi, M.: Online domain adaptation for semantic segmentation in ever-changing conditions. In: *ECCV (2022)* [4](#)
91. Parisi, G.I., Kemker, R., Part, J.L., Kanan, C., Wermter, S.: Continual lifelong learning with neural networks: A review. In: *Neural networks (2019)* [11](#)
92. Pellegrini, L., Graffieti, G., Lomonaco, V., Maltoni, D.: Latent replay for real-time continual learning. In: *IROS. IEEE (2020)* [10](#)
93. Podell, D., English, Z., Lacey, K., Blattmann, A., Dockhorn, T., Müller, J., Penna, J., Rombach, R.: Sdxl: Improving latent diffusion models for high-resolution image synthesis. *arXiv preprint arXiv:2307.01952* (2023) [4](#), [7](#), [9](#), [36](#), [40](#), [41](#)
94. Prabhu, A., Hammoud, H.A.A.K., Lim, S.N., Ghanem, B., Torr, P.H., Bibi, A.: From categories to classifier: Name-only continual learning by exploring the web. *arXiv preprint arXiv:2311.11293* (2023) [1](#), [2](#), [4](#), [33](#)
95. Prabhu, A., Torr, P.H., Dokania, P.K.: Gdumb: A simple approach that questions our progress in continual learning. In: *Computer Vision–ECCV 2020: 16th European Conference, Glasgow, UK, August 23–28, 2020, Proceedings, Part II 16*. pp. 524–540. Springer (2020) [4](#)
96. Quang, J.: Does training ai violate copyright law? *Berkeley Tech. LJ* **36**, 1407 (2021) [25](#)
97. Radford, A., Kim, J.W., Hallacy, C., Ramesh, A., Goh, G., Agarwal, S., Sastry, G., Askell, A., Mishkin, P., Clark, J., et al.: Learning transferable visual models from natural language supervision. In: *ICML. PMLR (2021)* [4](#), [8](#), [11](#), [33](#)
98. Ramasesh, V.V., Lewkowycz, A., Dyer, E.: Effect of scale on catastrophic forgetting in neural networks. In: *ICLR (2022)*, https://openreview.net/forum?id=GHVS8_yPeEa [14](#)

99. Razzhigaev, A., Shakhmatov, A., Maltseva, A., Arkhipkin, V., Pavlov, I., Ryabov, I., Kuts, A., Panchenko, A., Kuznetsov, A., Dimitrov, D.: Kandinsky: an improved text-to-image synthesis with image prior and latent diffusion. arXiv preprint arXiv:2310.03502 (2023) [4](#)
100. Rolnick, D., Ahuja, A., Schwarz, J., Lillicrap, T., Wayne, G.: Experience replay for continual learning. In: NeurIPS (2019) [4](#), [9](#), [11](#), [13](#), [24](#), [32](#)
101. Rombach, R., Blattmann, A., Lorenz, D., Esser, P., Ommer, B.: High-resolution image synthesis with latent diffusion models. In: CVPR (2022) [4](#)
102. Rosenfeld, A., Tsotsos, J.K.: Incremental learning through deep adaptation. In: TPAMI (2018) [4](#)
103. Russakovsky, O., Deng, J., Su, H., Krause, J., Satheesh, S., Ma, S., Huang, Z., Karpathy, A., Khosla, A., Bernstein, M., et al.: Imagenet large scale visual recognition challenge. In: IJCV (2015) [10](#)
104. Rusu, A.A., Rabinowitz, N.C., Desjardins, G., Soyer, H., Kirkpatrick, J., Kavukcuoglu, K., Pascanu, R., Hadsell, R.: Progressive neural networks. arXiv preprint arXiv:1606.04671 (2016) [13](#), [31](#), [32](#)
105. Sadat, S., Buhmann, J., Bradely, D., Hilliges, O., Weber, R.M.: Cads: Unleashing the diversity of diffusion models through condition-annealed sampling. arXiv preprint arXiv:2310.17347 (2023) [5](#)
106. Sato, R.: Active learning from the web. In: WWW (2023) [2](#)
107. Schuhmann, C., Beaumont, R., Vencu, R., Gordon, C., Wightman, R., Cherti, M., Coombes, T., Katta, A., Mullis, C., Wortsman, M., et al.: Laion-5b: An open large-scale dataset for training next generation image-text models (2022) [11](#), [25](#), [33](#)
108. Seo, M., Koh, H., Choi, J.: Budgeted online continual learning by adaptive layer freezing and frequency-based sampling. In: OpenReview (2024), <https://openreview.net/forum?id=3klVRLhK7w> [24](#)
109. Shanahan, M., Kaplanis, C., Mitrović, J.: Encoders and ensembles for task-free continual learning. arXiv preprint arXiv:2105.13327 (2021) [4](#)
110. Shi, Y., Peng, D., Liao, W., Lin, Z., Chen, X., Liu, C., Zhang, Y., Jin, L.: Exploring ocr capabilities of gpt-4v (ision): A quantitative and in-depth evaluation. arXiv preprint arXiv:2310.16809 (2023) [6](#), [34](#)
111. Shim, D., Mai, Z., Jeong, J., Sanner, S., Kim, H., Jang, J.: Online class-incremental continual learning with adversarial shapley value. In: AAAI (2021) [9](#), [11](#), [13](#), [24](#)
112. Shtedritski, A., Rupprecht, C., Vedaldi, A.: What does clip know about a red circle? visual prompt engineering for vlms. arXiv preprint arXiv:2304.06712 (2023) [6](#), [34](#)
113. Simon, C., Faraki, M., Tsai, Y.H., Yu, X., Schuler, S., Suh, Y., Harandi, M., Chandraker, M.: On generalizing beyond domains in cross-domain continual learning. In: CVPR (2022) [4](#)
114. Solatorio, A.V.: Gistembd: Guided in-sample selection of training negatives for text embedding fine-tuning. arXiv preprint arXiv:2402.16829 (2024), <https://arxiv.org/abs/2402.16829> [35](#)
115. Solon, O.: Facial recognition’s ‘dirty little secret’: Millions of online photos scraped without consent. In: NBC News. vol. 12 (2019) [25](#), [26](#)
116. Somepalli, G., Gupta, A., Gupta, K., Palta, S., Goldblum, M., Geiping, J., Shrivastava, A., Goldstein, T.: Measuring style similarity in diffusion models. arXiv preprint arXiv:2404.01292 (2024) [14](#)
117. Subramani, N., Luccioni, S., Dodge, J., Mitchell, M.: Detecting personal information in training corpora: an analysis. In: TrustNLP (2023) [26](#)

118. Sun, X., Leng, X., Wang, Z., Yang, Y., Huang, Z., Zheng, L.: Cifar-10-warehouse: Broad and more realistic testbeds in model generalization analysis. In: ICLR (2024) [10](#), [24](#), [31](#)
119. Sun, X., Zheng, L., Lai, Y.K., Yang, J.: Learning from web data: the benefit of unsupervised object localization. arXiv preprint arXiv:1812.09232 (2018) [2](#)
120. Tang, J., Nie, Y., Markhasin, L., Dai, A., Thies, J., Nießner, M.: Diffuscene: Scene graph denoising diffusion probabilistic model for generative indoor scene synthesis. arXiv preprint arXiv:2303.14207 (2023) [4](#)
121. Team, G., Anil, R., Borgeaud, S., Wu, Y., Alayrac, J.B., Yu, J., Soricut, R., Schalkwyk, J., Dai, A.M., Hauth, A., et al.: Gemini: a family of highly capable multimodal models. arXiv preprint arXiv:2312.11805 (2023) [6](#), [12](#), [34](#), [35](#)
122. Tian, Y., Fan, L., Chen, K., Katabi, D., Krishnan, D., Isola, P.: Learning vision from models rivals learning vision from data. arXiv preprint arXiv:2312.17742 (2023) [2](#), [4](#), [6](#)
123. Tian, Y., Fan, L., Isola, P., Chang, H., Krishnan, D.: Stablerep: Synthetic images from text-to-image models make strong visual representation learners. In: NeurIPS (2024) [4](#)
124. Tiwari, R., Killamsetty, K., Iyer, R., Shenoy, P.: Gcr: Gradient coreset based replay buffer selection for continual learning. In: CVPR (2022) [4](#)
125. Vanherle, B., Moonen, S., Van Reeth, F., Michiels, N.: Analysis of training object detection models with synthetic data. arXiv preprint arXiv:2211.16066 (2022) [1](#)
126. Verwimp, E., Yang, K., Parisot, S., Hong, L., McDonagh, S., Pérez-Pellitero, E., De Lange, M., Tuytelaars, T.: Clad: A realistic continual learning benchmark for autonomous driving. Neural Networks (2023) [3](#)
127. Wang, J., Lan, C., Liu, C., Ouyang, Y., Qin, T., Lu, W., Chen, Y., Zeng, W., Yu, P.: Generalizing to unseen domains: A survey on domain generalization. IEEE Transactions on Knowledge and Data Engineering (2022) [4](#)
128. Wang, Q., Fink, O., Van Gool, L., Dai, D.: Continual test-time domain adaptation. In: CVPR (2022) [4](#)
129. Wang, Z., Zhang, Z., Lee, C.Y., Zhang, H., Sun, R., Ren, X., Su, G., Perot, V., Dy, J., Pfister, T.: Learning to prompt for continual learning. In: CVPR (2022) [4](#)
130. Wenger, E., Li, X., Zhao, B.Y., Shmatikov, V.: Data isotopes for data provenance in dnns. arXiv preprint arXiv:2208.13893 (2022) [26](#)
131. Xu, W., Zhao, J., Iannacci, F., Wang, B.: Ffpdg: Fast, fair and private data generation. arXiv preprint arXiv:2307.00161 (2023) [26](#)
132. Xu, Z., Liu, Z., Yan, Y., Liu, Z., Xiong, C., Yu, G.: Cleaner pretraining corpus curation with neural web scraping. arXiv preprint arXiv:2402.14652 (2024) [2](#)
133. Xue, L., Constant, N., Roberts, A., Kale, M., Al-Rfou, R., Siddhant, A., Barua, A., Raffel, C.: mt5: A massively multilingual pre-trained text-to-text transformer. arXiv preprint arXiv:2010.11934 (2020) [25](#)
134. Yoon, J., Madaan, D., Yang, E., Hwang, S.J.: Online coreset selection for rehearsal-based continual learning. In: ICLR (2021) [4](#)
135. Yoon, J., Yang, E., Lee, J., Hwang, S.J.: Lifelong learning with dynamically expandable networks. In: ICLR (2018) [4](#)
136. Yuan, Y., Shi, C., Wang, R., Chen, L., Jiang, F., You, Y., Lam, W.: Mcqueen: a benchmark for multimodal conversational query rewrite. In: EMNLP (2022) [1](#)
137. Zenke, F., Poole, B., Ganguli, S.: Continual learning through synaptic intelligence. In: ICML. PMLR (2017) [4](#)
138. Zhang, D., Xia, B., Liu, Y., Xu, X., Hoang, T., Xing, Z., Staples, M., Lu, Q., Zhu, L.: Tag your fish in the broken net: A responsible web framework for protecting online privacy and copyright. arXiv preprint arXiv:2310.07915 (2023) [2](#)

139. Zhang, R., Isola, P., Efros, A.A., Shechtman, E., Wang, O.: The unreasonable effectiveness of deep features as a perceptual metric. In: Proceedings of the IEEE conference on computer vision and pattern recognition. pp. 586–595 (2018) [41](#)
140. Zhang, Y., Zhou, D., Hooi, B., Wang, K., Feng, J.: Expanding small-scale datasets with guided imagination. In: NeurIPS (2024) [4](#)
141. Zhao, Y., Xu, Y., Xiao, Z., Hou, T.: Mobilediffusion: Subsecond text-to-image generation on mobile devices. arXiv preprint arXiv:2311.16567 (2023) [4](#)
142. Zhou, D.W., Wang, Q.W., Ye, H.J., Zhan, D.C.: A model or 603 exemplars: Towards memory-efficient class-incremental learning. In: ICLR (2022) [4](#), [9](#), [11](#), [24](#)
143. Zhou, K., Yang, Y., Hospedales, T., Xiang, T.: Deep domain-adversarial image generation for domain generalisation. In: AAAI (2020) [3](#), [7](#), [9](#), [10](#), [13](#), [14](#), [24](#), [29](#), [30](#), [31](#)
144. Zhu, W., Hessel, J., Awadalla, A., Gadre, S.Y., Dodge, J., Fang, A., Yu, Y., Schmidt, L., Wang, W.Y., Choi, Y.: Multimodal c4: An open, billion-scale corpus of images interleaved with text. In: NeurIPS (2024) [25](#)

A Details about Experiment Setup

To set a domain generalization benchmark for a class incremental learning (class-IL) setup, we divide it into multiple disjoint tasks. Tasks do not share classes, since we assume a disjoint setup. We summarize the total number of classes per dataset, the number of classes per task, and the number of tasks in Table 6. Within each dataset, all tasks have the same size, except PACS, which has a total of 7 classes. For PACS, the first task includes 3 classes, while the subsequent tasks include data for 2 classes each.

Table 6: Task configurations for class-IL setup on each domain generalization dataset.

Dataset	total # of classes	# of tasks	# of classes / task
PACS [143]	7	3	2 (only initial task: 3)
DomainNet [84]	345	5	69
CIFAR-10-W [118]	10	5	2
CCT [12]	12	4	3

B Details of Baselines

Replay-based method. ER [100], DER [18], ASER [111], MIR [3], and X-DER [16] are methods that store previously encountered data in episodic memory and use them during future training to prevent forgetting. Since replay-based methods achieve strong performance, we chose many of them as baselines. ER, despite its simplicity, exhibits robust performance, as demonstrated in later studies [42, 108]. DER stores not only images and labels, but also logits in the form of triplets, distilling information about previous tasks through stored logits. X-DER is an extended version of DER, which addresses the logit outdated problem of DER through logit updates and future preparation. ASER and MIR retrieve training batches from episodic memory using adversarial shapely value and degree of interference, respectively, instead of random retrieval.

Regularization-based method. LiDER [15] addresses the challenge of poor generalization in online CL due to the instability of decision boundaries, using layer-wise Lipschitz constants. LiDER is a plug-and-play method that can be combined with other CL baselines. Given that the paper that introduced LiDER demonstrated that it achieved the best performance when integrated with X-DER [16], we presented the combined results of LiDER and X-DER as the performance of LiDER.

Architecture-based method. MEMO [142] is a network expansion approach in which the back-end layers are task-specific for each task, while the front-end layers are shared across tasks.

C Manual Annotation *vs.* Web-Scraping *vs.* Generative data

In modern deep learning, the trajectory of advancement is heavily influenced by the exponential growth of training data and the corresponding models trained on these vast datasets. Foundation models are typically exposed to datasets in the order of billions during training, obtained predominantly through web scraping [7, 19, 41, 64, 107, 133, 144]. Although web scraping is a cost-effective method to produce high-quality datasets, studies underscore issues such as potential biases [21, 39, 89], copyright, privacy, and license concerns [96, 115], and the risks of data contamination [31, 73] or data leakage from evaluation [8].

As demonstrated in Fig. 1, we highlight the key differences between Manually Annotated (MA), Web scraped, and Generated data on six different axes: (a) Controllability, (b) Storage issues, (c) Usage restrictions, (d) Privacy issues, (e) Acquisition cost, and (f) Noise. In this section, we aim to provide the definition of each of these axes and their corresponding implications on each type of data source.

Controllability encompasses the ability to generate or acquire images with various contexts, backgrounds, settings, and themes as desired. It pertains to the ability to obtain images depicting different concepts in compositions not commonly found in natural environments, as well as in domains relevant to the task at hand. Under this definition, we assert that the MA data exhibit low controllability. This limitation arises from its reliance on data captured from a finite set of scenarios or sensors, which inherently restricts the breadth of diverse settings where the concept can be observed. Web-scraped data also suffer from low controllability for the same reasons. In contrast, the generated data have high controllability due to the ability of foundation text-to-image (T2I) generators to produce diverse images for each concept through varied prompting.

Storage issues. Storing extensive data, locally or in the cloud, imposes additional costs, which can become impractical in environments constrained by limited total storage capacity. In addition, transmitting large, substantial data samples in a federated setup can face challenges arising from bandwidth and latency bottlenecks. In such contexts, depending on a large corpus of MA data becomes counterintuitive. On the other hand, both web-scraped and generated data present themselves as cost-effective alternatives for accessing substantial data volumes without necessitating explicit storage expenditures.

Usage restrictions encompass limitations imposed on the use of images for training machine/deep learning models, typically due to copyright or licensing protections. These restrictions arise from various legal frameworks across different demographics, regulating, and sometimes prohibiting, the training of models on protected data for commercial deployment. This challenge is particularly prevalent in web-scraped data, where the abundance of protected data may not be adequately filtered [58]. In contrast, MA data bypass this issue, as it is

presumed that the data are filtered or obtained from a proprietary source with appropriate permissions during annotation. Notably, generated data offer a more advantageous position, as they do not necessitate such filtering and encounter limited or no usage restrictions, thereby providing a readily available solution to issues arising from data protection concerns.

Privacy issues may arise when data samples inadvertently leak or explicitly contain sensitive, confidential, or private user information. Examples of such images could include those featuring people’s faces [82, 88] or personal objects that disclose identity-related details, such as addresses or financial assets. Once again, web data emerge as the primary source vulnerable to issues stemming from the use of private data, an issue extensively present in web-scraped data [77, 115, 117, 130]. MA data are expected to be protected from privacy concerns due to prior filtering or explicit agreement on data usage prior to annotation. In comparison, generated data should ideally not contain private data. Furthermore, several recent works [22, 24, 25, 131] have explored methods to enforce fairness and differential privacy in data synthesis, offering solutions for identity protection.

Acquisition cost refers to the total expenses incurred in obtaining a specific number of data samples necessary to train or evaluate the learner f_θ for a particular task. As emphasized in 1, MA data entail a substantial acquisition cost, primarily due to the expenses associated with densely annotating the data through human workers. This, coupled with the rigorous filtering process, makes MA data prohibitively expensive to acquire at scale. Although web data do not require such significant financial outlay for annotation, they do require intensive filtering, which contributes to an elevated cost and poses a barrier to constructing large datasets solely from web sources. In contrast, due to the advantages in controllability, generated data boast a notably low acquisition cost for generating large and diverse datasets.

Noise pertains to instances where data that are not related to a concept are erroneously labeled as belonging to that concept. It may also mean discrepancies between the context of the data and the associated concept. As highlighted in Sec. J, web data often exhibit a high degree of noise, necessitating extensive filtering or label correction processes. In contrast, both MA data and generated data are less susceptible to such noise. In the case of MA data, the presumption of prior filtering serves as a primary solution to mitigate noisy data. Meanwhile, for generated data, the advantages of controllability enable the mitigation of noise resulting from inconsistencies in concept-image alignment. Despite the drawback of requiring GPU usage, T2I model inference incurs lower costs compared to MA due to its ability to generate pure images, making it a more cost-effective option.

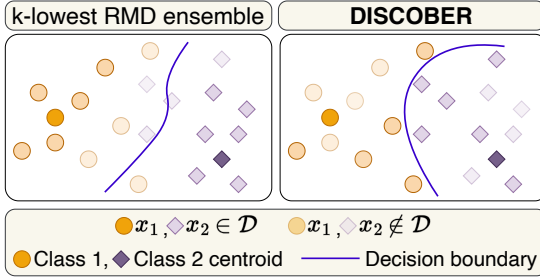


Fig. 7: DISCOBER helps in finding a tighter decision boundary due to having a higher probability of including high RMD scored samples in the ensemble of generated data \mathcal{D} . Intuitively, high RMD scored samples are farther away from their class prototype but closer to other class samples in comparison to low RMD scored samples which are concentrated closer around the class prototype. Note that DISCOBER includes not only high RMD samples but also some low RMD (*i.e.*, class-representative) samples.

D Details of RMD Score Calculation

The RMD [30] score of a sample (x_i, y_i) is defined as follows:

$$\begin{aligned} \mathcal{RMD}(x_i, y_i) &= \mathcal{M}_{cls}(x_i, y_i) - \mathcal{M}_{agn}(x_i), \\ \mathcal{M}_{cls}(x_i, y_i) &= -(G(x_i) - \mu_{y_i})^T \Sigma^{-1} (G(x_i) - \mu_{y_i}), \\ \mathcal{M}_{agn}(x_i) &= -(G(x_i) - \mu_{agn})^T \Sigma_{agn}^{-1} (G(x_i) - \mu_{agn}), \end{aligned} \quad (3)$$

where G represents the feature extractor, $\mathcal{M}_{cls}(x_i, y_i)$ denotes the Mahalanobis distance from $G(x_i)$ to the corresponding class mean vector $\mu_{y_i} = \frac{1}{N_i} \sum_{y_j=y_i} G(x_j)$, with N_i being the count of samples labeled as y_i , Σ^{-1} denotes the inverse of the averaged covariance matrix across classes. Furthermore, $\mathcal{M}_{agn}(x_i)$ represents the class-agnostic Mahalanobis distance, where μ_{agn} denotes the overall sample mean, and Σ_{agn}^{-1} denotes the inverse covariance for the class-agnostic case.

In the online CL setup, where data arrive in a continuous stream, it is not feasible to calculate μ and Σ of the entire dataset. Instead, a necessity arises to continuously update these statistical parameters to accommodate the dynamic nature of the incoming data stream.

Starting with the initially computed mean vector μ_{y_i} and the covariance matrix Σ from N samples, the arrival of a new sample x_{N+1} triggers an update. The updated mean vector μ_{new} is computed incrementally using a simple moving average (SMA), as follows:

$$\mu_{new} = \frac{N\mu_{old} + x_{N+1}}{N + 1}. \quad (4)$$

Similarly, we calculate Σ using a simple moving variance. Specifically, the update for the new covariance matrix Σ_{new} is calculated using the deviation of the new sample from the old mean $\Delta = x_{N+1} - \mu_{old}$, and its deviation from the new mean $\Delta_{new} = x_{N+1} - \mu_{new}$.

Formally, we formulate the update process as follows:

$$\Sigma_{\text{new}} = \frac{1}{N+1} (N\Sigma_{\text{old}} + \Delta\Delta_{\text{new}}^T). \quad (5)$$

The update process for the class-agnostic mean vector μ_{agn} and covariance Σ_{agn} follows the same incremental approach as described for the class-specific components.

DISCOBER includes a significant number of samples with high RMD scores in the ensemble dataset. Not only does it include samples with the highest RMD scores, but it also probabilistically incorporates samples with low RMD scores. This approach ensures a core-set ensemble, and we illustrate the effect of DISCOBER in Fig. 7

E Comparison of Ensemble Methods

To validate the effect of DISCOBER on the generated data, we compare various ensemble methods in various continual learning methods and summarize in Tab. 7. While several ensemble methods have lower performance than *No ensembling*, which refers to the usage of images generated exclusively through SDXL, DISCOBER consistently outperforms other ensemble methods and *No ensembling* in both ID and OOD performance.

F Effect of DISCOBER in Web Data

To assess the impact of DISCOBER, a proposed RMD score-based probabilistic ensemble method, we conduct comparisons with various ensemble methods on web-scraped PACS data within various continual learning methods, and summarize the results in Tab. 8.

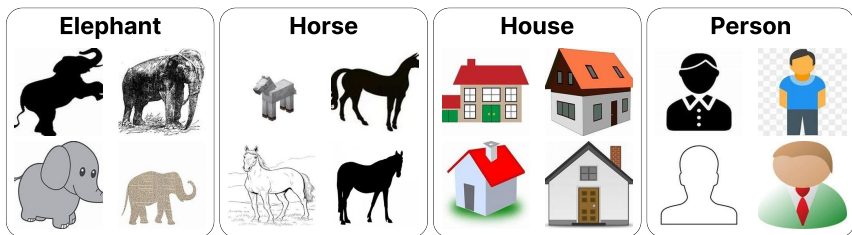


Fig. 8: While the average RMD scores for the elephant, horse, house, and person classes in web-scraped PACS data are 0.432, -0.231, 0.947, and -2.362, respectively, the samples depicted in the figures have average RMD scores of 2.727, 1.212, 3.273, and 0.331 for the same classes, respectively. Qualitatively, it is evident that web-scraped samples having different domains from the *Photo* domain of the PACS dataset tend to have relatively high RMD scores.

While DISCOBER always outperforms other ensemble methods in generated data, as shown in Tab. 1 and Tab. 7, in web-scraped data, the k -highest RMD

Table 7: Comparison of ensemble methods in PACS [143], using various CL methods for all ensemble methods. The proposed ensemble method outperforms other ensemble methods.

Methods Ensemble Method Δ		ID		OOD	
		$A_{AUC} \uparrow$	$A_{I_{ast}} \uparrow$	$A_{AUC} \uparrow$	$A_{I_{ast}} \uparrow$
ER	None (Baseline)	47.95±2.20	45.58±4.00	34.11±1.33	28.13±1.69
	Equal weight ensemble	48.00±1.71	44.04±3.75	32.97±1.25	25.32±1.79
	k -highest RMD ensemble	53.01±2.25	51.94±2.97	34.21±1.42	26.12±0.70
	k -lowest RMD ensemble	34.32±1.97	23.86±3.29	26.56±1.80	15.28±1.79
	Inverse Prob	43.37±2.47	37.63±3.82	30.11±1.32	23.41±0.79
	DISCOBER (Ours)	53.23±2.96	50.68±2.68	35.69±1.62	30.09±1.42
MIR	None (Baseline)	50.46±2.18	49.62±3.43	34.36±1.82	28.02±1.16
	Equal weight ensemble	45.62±5.11	43.68±4.61	31.11±2.90	24.62±2.28
	k -highest RMD ensemble	54.02±3.04	53.47±2.22	34.72±1.02	28.99±1.63
	k -lowest RMD ensemble	30.32±2.47	25.52±2.20	25.90±1.27	15.06±1.67
	Inverse Prob	38.88±3.00	33.95±2.41	27.90±1.69	20.02±2.19
	DISCOBER (Ours)	54.28±3.84	55.31±1.05	37.42±1.80	33.90±0.93
ASER	None (Baseline)	48.28±0.67	45.40±2.95	33.76±1.20	25.48±1.94
	Equal weight ensemble	47.10±3.47	43.20±3.54	31.82±1.60	25.41±1.33
	k -highest RMD ensemble	51.36±2.49	47.90±1.47	32.99±0.80	28.63±2.06
	k -lowest RMD ensemble	33.60±2.56	22.08±1.83	26.31±2.40	17.06±1.54
	Inverse Prob	41.84±2.10	32.28±2.63	28.33±1.20	20.78±1.43
	DISCOBER (Ours)	48.78±1.65	47.94±2.07	35.07±1.46	31.58±2.09
LiDER	None (Baseline)	51.74±2.48	50.40±2.79	34.04±1.90	27.10±1.41
	Equal weight ensemble	46.07±2.90	40.00±3.17	30.60±2.38	22.27±1.15
	k -highest RMD ensemble	51.60±2.18	50.80±4.30	31.59±1.67	25.03±1.62
	k -lowest RMD ensemble	33.06±2.41	22.14±3.02	24.94±1.17	13.52±1.01
	Inverse Prob	42.47±2.56	27.71±1.30	27.52±1.71	19.14±1.93
	DISCOBER (Ours)	52.46±3.11	51.35±5.26	36.18±1.44	30.94±1.24

ensemble outperforms DISCOBER, especially in OOD performance. This is because, unlike generated data, web-scraped data inherently contain samples from various domains, which may have high RMD scores, as shown in Fig. 8.

Specifically, during evaluation, we use the test set of the *Photo* domain in PACS as the ID test data, we employ data of the remaining domains (*Art Painting*, *Cartoon*, and *Sketch*) as the OOD test data. Despite considering the *Art Painting*, *Cartoon*, and *Sketch* domains as OOD domains, the k -highest RMD ensemble might incorporate more data from these domains into the training set compared to other ensemble methods, as data from these domains tend to have relatively high RMD scores. As a result, the k -highest RMD ensemble tends to outperform DISCOBER in OOD domains due to the nature of the web data, which includes samples from diverse domains. However, DISCOBER still outperforms the k -highest RMD ensemble in the ID domain.

Table 8: Comparison of ensemble methods in web-scraped data using categories of PACS [143] for various ensemble methods. For filtering, we filter out 80% of the samples with the lowest 80% clip scores from larger web-scraped data, which is 5 times larger than the manually annotated data.

Method	Ensemble Method Δ	ID		OOD	
		$A_{AUC} \uparrow$	$A_{last} \uparrow$	$A_{AUC} \uparrow$	$A_{last} \uparrow$
ER	None (Baseline)	53.18±2.73	52.11±2.57	29.01±2.17	24.70±0.83
	Equal weight ensemble	58.36±3.23	57.69±0.74	30.45±1.23	23.43±3.18
	k -highest RMD ensemble	60.07±3.14	58.22±3.22	32.02±1.36	29.37±1.54
	k -lowest RMD ensemble	54.76±3.33	54.90±1.24	30.96±1.45	25.73±2.06
	Inverse Prob	56.78±2.81	52.34±1.54	31.46±1.35	24.98±2.43
	DISCOBER (Ours)	60.25±2.78	60.30±2.84	29.07±1.04	26.96±0.65
ASER	None (Baseline)	50.12±3.32	42.49±4.06	27.50±1.92	19.04±1.48
	Equal weight ensemble	55.45±4.19	50.98±2.01	28.67±2.04	22.87±1.68
	k -highest RMD ensemble	59.15±3.41	56.38±2.97	32.22±1.49	25.57±1.73
	k -lowest RMD ensemble	50.79±4.18	44.93±1.86	28.75±1.79	23.68±1.22
	Inverse Prob	57.17±3.02	54.42±2.02	32.16±1.06	25.43±0.88
	DISCOBER (Ours)	60.30±3.49	63.32±1.83	29.98±0.66	25.09±0.80

G RMD Ablation

Table 9: Average RMD score for meta prompts. For each meta prompt, we generate four prompt rewrites. The average RMD score refers to the average of RMD scores obtained from all images generated using each meta prompt and its corresponding rewritten prompts.

Meta prompt	Average RMD score
A black and white image of [concept] highlighting dramatic contrasts.	-3.471
A minimalist image of [concept] using clean lines and muted colors.	-1.153
A photo of [concept] in analogous colors.	-0.618
A photo of [concept] in complementary colors.	-1.216
A photo of [concept] in earth tones.	1.568
A photo of [concept] in neutral tones.	1.779
This is an image of the [concept].	0.492
A realistic image of [concept].	1.203
A vintage photograph of [concept] with a warm, faded aesthetic.	2.425
A high-resolution photo of [concept] capturing fine details.	-0.446

We calculate the RMD score for each meta-prompt and summarize the results in Tab. 9. Based on the varied distribution of RMD scores for each meta-prompt, it can be observed that using a diversified set of prompts, rather than a single prompt, allows for the generation of samples ranging from easy to difficult. In other words, it ensures a broader coverage of the sample difficulty spectrum,

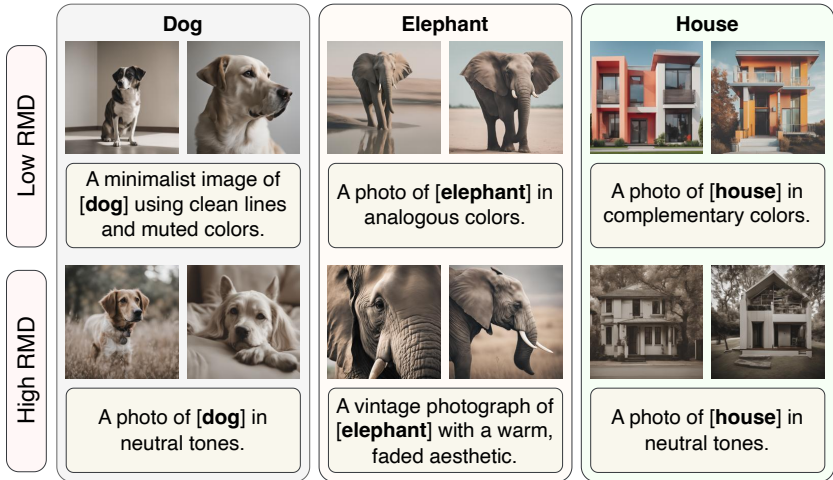


Fig. 9: Examples of generated images representing the concepts "Dog," "Elephant," and "House" from the PACS dataset [143]. The images in the top row are generated from meta-prompts with low RMD scores, while the images in the bottom row are generated from meta-prompts with high RMD scores.

capturing a more comprehensive representation of the underlying data characteristics.

In addition, we illustrate samples generated from prompts for low RMD samples and high RMD samples in Fig. 9.

H Scaling behavior

As examining the behavior of in-distribution (ID) accuracy and out-of-distribution (OOD) accuracy with respect to the volume of PACS generated data in Sec. 4.5, we also empirically analyze the scaling behavior in the CCT dataset in Fig. 10. When using both ResNet-18 and ViT as the backbone architecture, the OOD and ID performance increases linearly with the volume of generated data. It shows that with sufficient computational resources to generate more data, it is possible to achieve good performance without any manually annotated data.

I Experimental Results on CIFAR-10-W using ViT

We compared manually annotated (MA) data and generated data using DISCOBER with Vision Transformer (ViT) [104] as the backbone architecture on CIFAR-10-W [118]. As mentioned in Sec. 4.2, since CIFAR-10-W consists of only two domains, both are used to evaluate the out-of-distribution (OOD) domain. Additionally, since CIFAR-10-W is a web-scraped dataset, the domain of CIFAR-10-W and the web-scraped data are the same. Therefore, we excluded

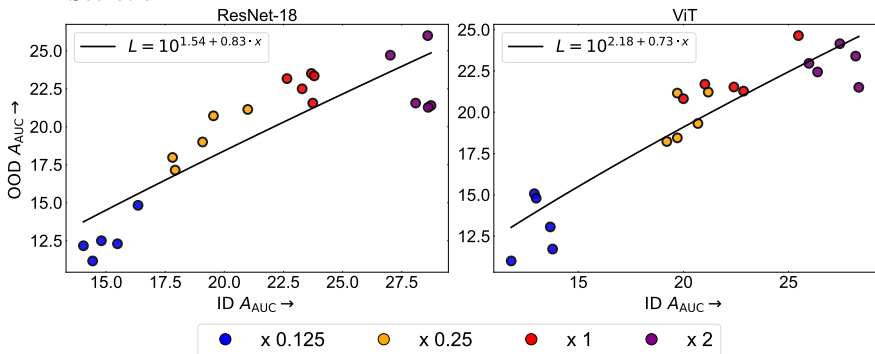


Fig. 10: Ensemble scaling behavior of (a) ResNet-18 [48] and (b) ViT [104] for ID A_{AUC} vs. OOD A_{AUC} on the CCT dataset [12] using ER [100]. (x 1) denotes the ensemble volume in primary experiments, the default data budget. web-scraped data in experiments on CIFAR-10-W and only evaluated OOD performance. We summarize the results in Tab. 10.

Table 10: Comparison of Manually Annotated (MA) data and DISCOBER on CIFAR-10-W. We use ViT as the backbone.

Method	Training Data	$A_{AUC} \uparrow$	$A_{last} \uparrow$
ER	DISCOBER	43.70±0.60	26.55±1.01
	MA	42.31±1.15	24.81±1.20
ER-MIR	DISCOBER	38.30±0.82	17.79±1.13
	MA	32.69±1.39	16.06±1.73
DER++	DISCOBER	38.31±0.82	17.80±1.13
	MA	36.54±1.15	16.91±1.02
ASER	DISCOBER	43.67±0.49	25.83±1.19
	MA	42.48±1.14	24.24±1.23
MEMO	DISCOBER	36.60±1.09	16.24±0.65
	MA	34.15±0.35	14.20±0.62

J Details about Web-Scraping

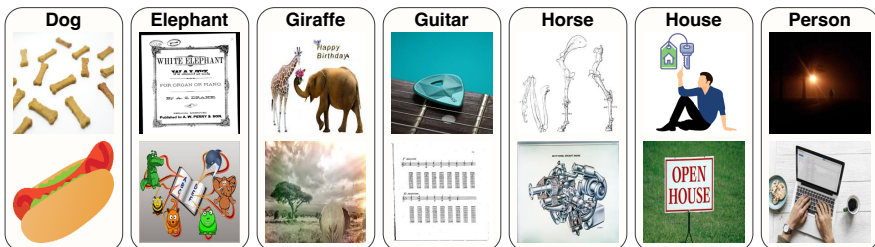


Fig. 11: Examples of noisy raw data obtained via web-scraping for the classes in the PACS dataset.

For the collection of our web dataset, we use three search engines: Flickr, Google, and Bing. To ensure a stable collection, we separate the process into querying (collecting URLs) and downloading. Specifically, for Flickr, we use its official API⁸ to collect URLs. However, since Google and Bing do not offer official image search APIs, utilize the publicly available querying tool⁹ to collect URLs, following [94]. Taking into account the possible errors in the URLs or the download process, we gather URLs corresponding to 1.4 times larger than we need. After collecting the URLs from each search engine, we use a multi-threaded downloader¹⁰ to quickly download the images, following [94].

For Flickr, we are able to download approximately 500 images per minute due to the rapid URL collection facilitated by the official API. Meanwhile, for Google and Bing, the download rate is slower, at approximately 100 images per minute on a single CPU machine. However, the download rate depends on network conditions, as well as the status of the API and the search engine.

Datasets scraped from search engines such as Flickr, Google, and Bing contain uncurated (*i.e.*, noisy) samples. To clean these datasets, following [107], we use a pre-trained CLIP [97] model to measure the similarity between the images and corresponding prompts. Specifically, we scraped 10% more data than the required dataset size (*i.e.*, the number of manually annotated data) and removed samples with a low CLIP similarity score for each experiment. Although prior work [94] addressed the ambiguity of queries through manual query design, such as adding an auxiliary suffix to refine queries, in an online CL scenario, where new concepts stream in real-time, such hand-crafted query designs for each concept are limited.

In summary, data noise, network dependency, and the need for manual query design specific to each concept restrict the use of web-scraped data in real-world scenarios where new concepts are encountered in real-time.

K Prompt Refiner Module ψ

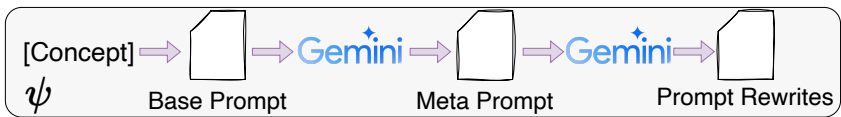


Fig. 12: Prompt Refiner Module (ψ): Given a [concept], ψ utilizes a pretrained frozen LLM to generate fine-grained prompt-rewrites in a two-step process.

The prompt refiner module (ψ) is a crucial component within our proposed **G-NoCL** framework. With the observed limited diversity in images generated from the same base prompt using a Text-to-Image (T2I) generator, the primary objective of ψ is to facilitate fine-grained prompt rewrites, thereby enhancing the diversity of the generated images. These prompt rewrites aim to cover a

⁸<https://www.flickr.com/services/api/flickr.photos.search.html>

⁹<https://github.com/hellock/icrawler>

¹⁰<https://github.com/rom1504/img2dataset>

broad spectrum of the $[concept]$ by considering various settings, backgrounds, and texture details.

As mentioned in 3.1, a novel concept is conveyed as a stream input to ψ . This $[concept]$ is then transformed into the base prompt following the template: "*This is an image of the [concept]*", a prompt widely used in existing studies [110, 112]. Subsequently, we rewrite 10 different prompts, named *meta-prompts*, using the base prompt and the Gemini [121] Language Model (LLM). Next, we generate four rewritten prompts per each meta-prompt using the Gemini, resulting in a total set of 50 prompts. These 50 prompts serve as queries for the T2I generators \mathcal{G} . It is important to note that our proposed end-to-end framework operates in a zero-shot manner *i.e.*, it does not involve gradient-based training. Furthermore, the prompts, which have been rewritten using the Gemini, are used as-is without any manually selection process.

When designing ψ , two key aspects need to be considered: (i) choosing the appropriate Language Model (LLM) and (ii) deciding on the number of stages for prompt rewrite generation.

K.1 LLM selection

Meta-prompts We consider two prominent Large Language Models (LLMs) for integration into the ψ module: (i) GPT-3.5 [17], and (ii) Gemini [121]. To select the appropriate LLM, we compare the quality, diversity, and applicability of the meta-prompts generated from the same base prompt using both LLMs.

The meta-prompts generated by GPT-3.5 are as follows:

1. "Generate an image representing $[concept]$."
2. "This is an image of what? - $[concept]$ "
3. "Show me a visual depiction of $[concept]$."
4. "Create an artistic representation for $[concept]$."
5. "Generate an image that encapsulates the essence of $[concept]$."
6. "Produce a visual interpretation corresponding to $[concept]$."
7. "Illustrate $[concept]$ in the form of an image."
8. "What does an image portraying $[concept]$ look like?"
9. "Create a visual concept for $[concept]$."
10. "Generate an artistic rendering reflective of $[concept]$."

Unlike GPT-3.5, Gemini generates more diversified prompts, since it supports a wide range of background & setting. The meta-prompts generated by Gemini are as follows:

1. Style & Detail:
 - (a) **High-resolution photo:** A high-resolution photo of $[concept]$ capturing fine details.
 - (b) **Photorealistic:** A realistic image of $[concept]$.
 - (c) **Vintage:** A vintage photograph of $[concept]$ with a warm, faded aesthetic.

- (d) **Black and White:** A black and white image of [concept] highlighting dramatic contrasts.
 - (e) **Minimalist:** A minimalist image of [concept] using clean lines and muted colors.
2. Color & Pattern:
- (a) **Analogous colors:** A photo of [concept] in analogous colors.
 - (b) **Complementary colors:** A photo of [concept] in complementary colors.
 - (c) **Earth tones:** A photo of [concept] in earth tones.
 - (d) **Neutral tones:** A photo of [concept] in neutral tones.

Table 11: Average cosine similarity of normalized embeddings of the meta-prompts generated via GPT-3.5 [17] and Gemini [121] evaluated using standard sentence embedding models [38, 44, 85, 114]. **Lower** similarity score indicates **higher** diversity in the meta-prompts.

LLM	GISTEmbed-L [114]	mxbai-embed-L ¹¹	Sentence-T5-B [85]	LaBSE [38]	Jina-v2 [44]
GPT-3.5 [17]	0.8552	0.8811	0.944	0.7602	0.9089
Gemini [121]	0.8088	0.8544	0.9137	0.7187	0.8987

We observe that Gemini provides a more diverse set of meta-prompts in comparison to the ones provided by GPT-3.5, which appear to be rather rephrasing of the original base-prompt excluding a few like "*Generate an artistic rendering reflective of [concept].*" Furthermore, we assess the intra-similarity of the meta-prompts generated by GPT-3.5 and Gemini by calculating the average cosine similarity using normalized embeddings generated by state-of-the-art sentence embedding models, and summarize the results in Table 11. The results show that Gemini consistently achieves a lower average cosine similarity compared to GPT-3.5. In other words, Gemini demonstrates higher diversity in its generated meta-prompts. Therefore, we use the meta-prompts generated by Gemini.

Prompt Rewrites Based on the 10 meta-prompts provided by the Gemini model (K.1), we try to rewrite each meta-prompt four distinct ways via Gemini. Effective prompt rewrites play a pivotal role in enhancing diversity among the images generated within the same meta-prompts, as illustrated in Fig. 13. Therefore, the construction of well-crafted prompt rewrites from the predefined meta-prompts is essential.

Note: Along with the 9 meta-prompts, we also use the base-prompt to generate four corresponding prompt rewrites.

The following are the prompt-rewrites provided by Gemini:

- 1. **Original Prompt:** A black and white image of [concept] highlighting dramatic contrasts.

¹¹<https://www.mixedbread.ai/blog/mxbai-embed-large-v1>

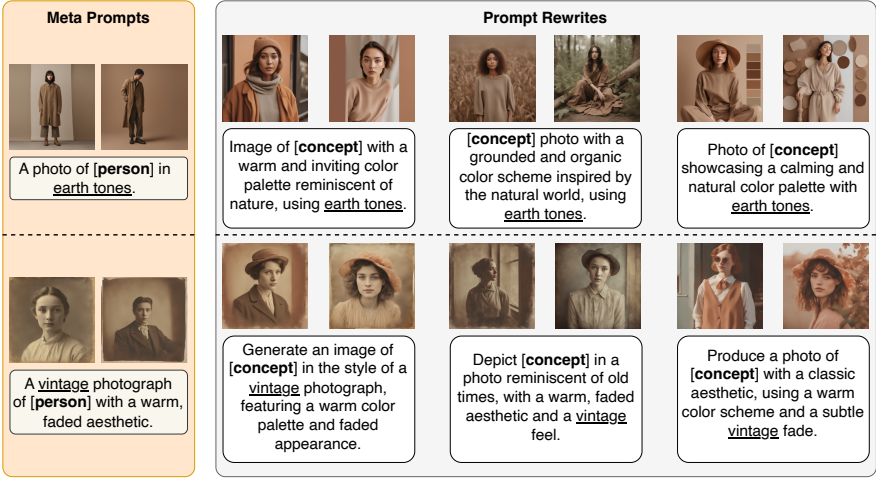


Fig. 13: Diversity in generated images using three prompt rewrites of two selected meta prompts for the concept - "person" using SDXL [93].

- (a) High-contrast black and white photo of [concept] emphasizing dramatic lighting.
 - (b) Black and white [concept] image with bold contrasts, showcasing its form.
 - (c) Black and white [concept] photography capturing stark shadows and highlights.
 - (d) Dramatic black and white image of [concept] with deep blacks and bright whites.
2. **Original Prompt:** A minimalist image of [concept] using clean lines and muted colors.
 - (a) Simple and elegant photo of [concept] featuring clean lines and muted tones.
 - (b) Minimalist composition of [concept] with clean lines and a subdued color palette.
 - (c) Uncluttered image of [concept] using clean lines and muted colors for a serene look.
 - (d) Photo of [concept] with a minimalist aesthetic, featuring clean lines and soft colors.
 3. **Original Prompt:** A photo of [concept] in analogous colors.
 - (a) [concept] photo featuring a harmonious blend of analogous colors.
 - (b) Image of [concept] showcasing a cohesive color scheme using analogous colors.
 - (c) Photo of [concept] where the colors naturally complement each other, following an analogous color scheme.
 - (d) [concept] image with a pleasing color palette using analogous colors that sit next to each other on the color wheel.
 4. **Original Prompt:** A photo of [concept] in complementary colors.

- (a) Image of [concept] featuring contrasting yet balanced colors, using a complementary color scheme.
 - (b) Photo of [concept] where the colors create a sense of visual tension through complementary colors.
 - (c) [concept] image with a vibrant color palette using complementary colors that sit opposite each other on the color wheel.
 - (d) Photo of [concept] showcasing a dynamic color combination with complementary hues.
5. **Original Prompt:** A photo of [concept] in earth tones.
- (a) Photo of [concept] featuring natural, earthy colors like brown, green, and beige.
 - (b) Image of [concept] with a warm and inviting color palette reminiscent of nature, using earth tones.
 - (c) [concept] photo with a grounded and organic color scheme inspired by the natural world, using earth tones.
 - (d) Photo of [concept] showcasing a calming and natural color palette with earth tones.
6. **Original Prompt:** A photo of [concept] in neutral tones.
- (a) Photo of [concept] featuring a subtle and timeless color palette with neutral tones.
 - (b) Image of [concept] with a classic and versatile color scheme using neutral tones.
 - (c) [concept] photo with a sophisticated and understated color palette dominated by neutral tones.
 - (d) Photo of [concept] where the focus falls on the subject itself through the use of neutral tones.
7. **Original Prompt (Base):** This is an image of the [concept]
- (a) Capture a stunning image of [concept].
 - (b) Showcase the beauty of [concept] in a photo.
 - (c) Create a photo that portrays [concept] accurately.
 - (d) Generate a visually appealing image of [concept].
8. **Original Prompt:** A realistic image of [concept].
- (a) Create a lifelike image of [concept] that captures its true essence.
 - (b) Generate a photo of [concept] that appears true to life.
 - (c) Produce an image of [concept] with realistic details and lighting.
 - (d) Depict [concept] in a photo with a high degree of visual realism.
9. **Original Prompt:** A vintage photograph of [concept] with a warm, faded aesthetic.
- (a) Create a nostalgic photo of [concept] with a warm, vintage tone and faded colors.
 - (b) Generate an image of [concept] in the style of a vintage photograph, featuring a warm color palette and faded appearance.
 - (c) Produce a photo of [concept] with a classic aesthetic, using a warm color scheme and a subtle vintage fade.
 - (d) Depict [concept] in a photo reminiscent of old times, with a warm, faded aesthetic and a vintage feel.

10. **Original Prompt:** A high-resolution photo of [concept] capturing fine details.
 - (a) Close-up photo of [concept] in high resolution, revealing intricate details.
 - (b) Detailed, high-resolution image of [concept] showcasing its intricate features.
 - (c) Sharp, high-resolution photo of [concept] capturing every minute detail.
 - (d) Crystal clear photo of [concept] in high resolution, showing fine textures and patterns.

K.2 Number of Prompt Rewrite Stages

In an effort to illustrate the rationale behind the two-step process, creating meta-prompts and then rewriting each meta-prompt into multiple prompts, in ψ , we explore the single-step generation, which directly generates a complete set of prompt rewrites from the base prompt using the Gemini model.

The prompts generated through single-step generation are as follows:

1. **Direct phrasing:**
 - (a) Depict [concept].
 - (b) Generate an image of [concept].
 - (c) Show me a picture of [concept].
 - (d) Create a visual representation of [concept].
 - (e) Display an image containing [concept].
2. **Descriptive phrasing:**
 - (a) A photorealistic image of a [concept].
 - (b) A detailed illustration of a [concept].
 - (c) A high-resolution picture of a [concept] in its natural habitat.
 - (d) A close-up image of a [concept], showcasing its intricate details.
 - (e) A vibrant painting depicting a [concept] in action.
3. **Action-oriented phrasing:**
 - (a) Capture the essence of a [concept] in an image.
 - (b) Bring a [concept] to life with a stunning image.
 - (c) Showcase the beauty of a [concept] in a captivating image.
 - (d) Visualize a [concept] using your creative vision.
 - (e) Generate an image that embodies the concept of [concept].
4. **Context-specific phrasing:**
 - (a) Imagine a [concept] exploring a bustling city.
 - (b) Depict a [concept] resting peacefully in a serene landscape.
 - (c) Capture the playful energy of a [concept] in an image.
 - (d) Generate an image of a [concept] interacting with its environment.
 - (e) Showcase the unique characteristics of a [concept] in detail.
5. **Emotional phrasing:**
 - (a) Generate an image that evokes the majesty of a [concept].
 - (b) Capture the tranquility of a [concept] in its natural habitat.
 - (c) Showcase the playful joy of a [concept] in motion.
 - (d) Depict the power and strength of a [concept] visually.

- (e) Generate an image that captures the essence of a [concept]’s beauty.
6. **Figurative language:**
 - (a) Paint a picture of a [concept] coming to life.
 - (b) Sculpt a visual representation of a [concept].
 - (c) Weave a tapestry depicting the image of a [concept].
 - (d) Compose a portrait of a [concept] in its element.
 - (e) Capture the essence of a [concept] through the lens of imagination.
 7. **Storytelling:**
 - (a) Tell the story of a [concept] through a captivating image.
 - (b) Unfold a narrative around a [concept] through visual storytelling.
 - (c) Generate an image that sparks a story about a [concept].
 - (d) Capture a moment in the life of a [concept] with a stunning image.
 - (e) Showcase the journey of a [concept] through a series of images.
 8. **Additional variations:**
 - (a) A photo of [concept] in its natural environment.
 - (b) A vintage postcard depicting [concept].
 - (c) A pixel art rendition of [concept].
 - (d) A sketch capturing the essence of [concept].
 - (e) A classic painting style interpretation of [concept].
 - (f) A hyper-realistic image of [concept].
 - (g) A watercolor painting capturing the serenity of a [concept].
 - (h) A futuristic illustration of a [concept].
 - (i) A surreal depiction of a [concept] in a dreamlike setting.
 - (j) An animated GIF showcasing the movement of a [concept].
 - (k) A close-up portrait of a [concept] with its unique features highlighted.
 - (l) A panoramic view showcasing the vastness of a [concept]’s habitat.
 - (m) A minimalist interpretation of [concept] using simple lines and shapes.
 - (n) An abstract representation of the essence of [concept] using color and form.
 - (o) A photo of a [concept] interacting with humans (if applicable).

Although several prompts, rewritten using the base prompt, exhibit qualitative merit, a considerable number of them lack universal applicability across diverse concepts. For instance, prompts generated under context-specific phrasing, such as "Imagine a [concept] exploring a bustling city", generate only images related to a particular domain, which could potentially harm domain generalization performance.

In the future, as LLMs advance and better approaches for prompt diversification are proposed, we expect more diversified images to be generated, increasing the utility of G-NoCL.

L Analyzing Diversity of Generated Images

Our objective is to determine the impact of diversified prompts (**Meta prompts** and **Prompt rewrites**) on enhancing the diversity of the generated images. Using the prompt refiner module (see Appendix K), we produce a variety of

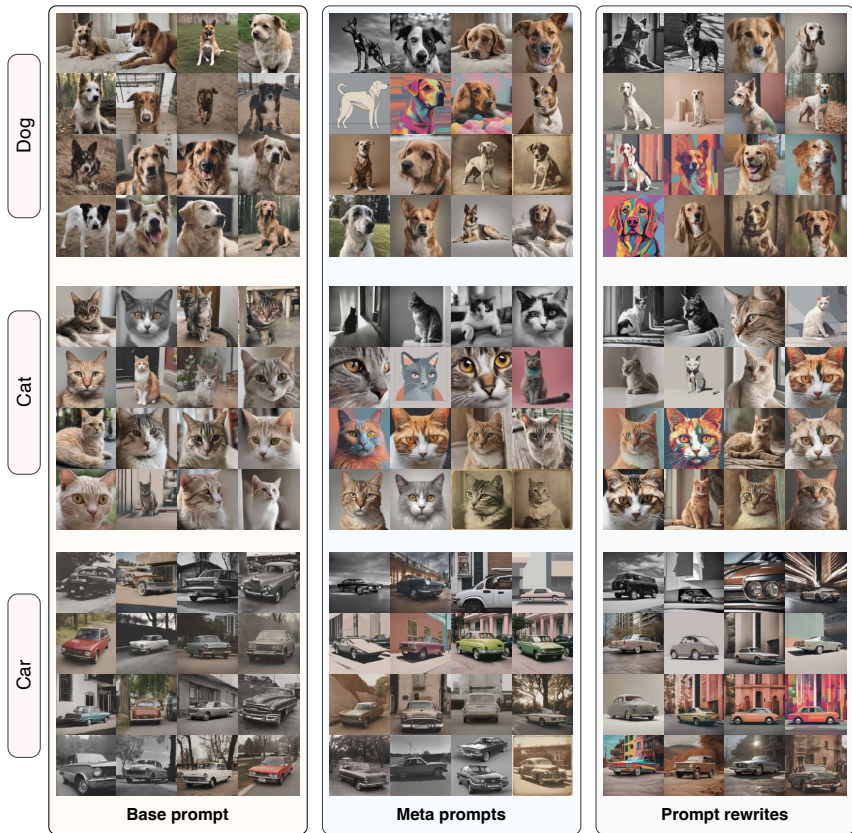


Fig. 14: Visualization of 16 randomly drawn samples generated via **Base Prompt**, **Meta Prompts**, and, **Prompt Rewrites** using SDXL [93] for three different classes - "Dog", "Cat", and, "Car" of the CIFAR-10 [67] dataset. Qualitatively, through observation, samples generated via **Meta Prompts** and **Prompt Rewrites** encompass more domains like: **Black and White**, **animated**, and, **vintage style**, in comparison to those generated by **Base Prompt** which usually have similar color profile without much variation in style.

prompts, thereby achieving a broader coverage of the target concept across different domains for the generated images. This approach differs from solely relying on the **Base prompt** to generate the entire image set while adhering to the specified data budget.

To validate the effectiveness of our proposed prompt diversification, we generate the CIFAR-10 datasets using three different prompting strategies (**Base prompt**, **Meta prompts** and **Prompt rewrites**) for subsequent evaluations, each class comprising 220 generated images. In Fig. 14, we present a qualitative comparison between the images generated using the **Base prompt** and those generated employing the **Meta prompts** and **Prompt rewrites**, utilizing the SDXL model [93] on the CIFAR-10 dataset [67]. We observe that images generated with the **Base prompt** exhibit a limited range of styles and color palettes, a con-

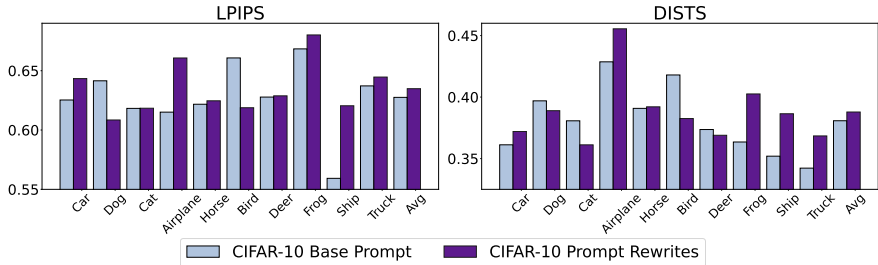


Fig. 15: Average pairwise image similarity of samples generated via **Base Prompt** and **Prompt Rewrites** using SDXL [93], measured by (a) LPIPS [139] and (b) DISTS [33] for classes in the CIFAR-10 [67] dataset. **Lower** values indicate **higher** average pairwise image similarity.

trast more pronounced in images generated with the **Meta prompts** and **Prompt rewrites**. The latter set of images, prompted diversely, encompass stylistic variations such as animations, black-and-white renditions, neutral tones, and vintage aesthetics. This visual diversity is further corroborated by the performance improvement demonstrated in Table 3, indicating improved results beyond those achieved solely by data generation with the **Base prompt**.

Furthermore, we calculate the average pairwise image similarity between samples generated using the **Base prompt** and those generated with **Prompt rewrites**, utilizing the LPIPS [139] and DISTS [33] metrics. As illustrated in Fig. 15, images produced through **Prompt rewrites** exhibit, on average, lower pairwise similarity, indicating a higher degree of diversity in generation compared to those generated solely with the **Base prompt**. We believe that the marginal difference of similarity arises from the fact that conventional image similarity metrics such as LPIPS and DISTS calculate similarity primarily based on feature representation distance, without explicitly considering the variance in image domain and style.

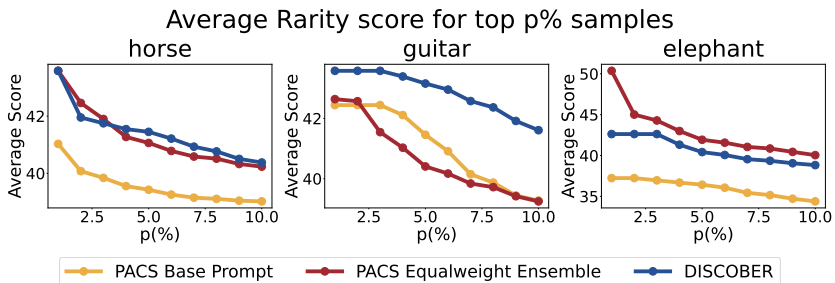


Fig. 16: Average Rarity score for horse, guitar, and elephant class in the PACS dataset.

To validate the diversity of a set ensembled using our proposed method, named DISCOBER, we compare three approaches: **Base Prompt**, **Equal-weight Ensemble**, and **DISCOBER**, using the Rarity score metric [45], a metric that evalu-

ates the uncommonness of the generated data. As shown in Fig. 16, DISCOBER consistently achieves higher Rarity scores compared to data generated solely with the **Base Prompt**, while the **Equal-weight Ensemble** yields lower Rarity scores, particularly in the **guitar** class. This is because the **Equal-weight Ensemble** fails to consider the overlap of the data generated by each generator during ensembling, which could result in a decrease in the diversity of the ensemble set. Note that DISCOBER does not consistently achieve higher Rarity scores than **Equal-weight Ensemble** (e.g., **elephant** class). This is because DISCOBER not only incorporates samples with high RMD scores but also includes a small portion of samples with low RMD scores for coresets selection.